BIOMOLECULAR RECOGNITION OF SOME BIOACTIVE COMPOUNDS IN SPICES WITH AMYLOID-BETA PRECURSOR PROTEIN

PROJECT REPORT

Submitted to **Kannur University**

In Partial Fulfilment of the Requirements for the award of the degree of

MASTER OF SCIENCE IN PHYSICS

Submitted by

KRISHNA SAGAR N

Reg No: C1PSPH1603

UNDER THE GUIDANCE OF

Dr. HARIS P

Assistant Professor
Department of
Physics, Sir Syed
College,
Taliparamba

POST GRADUATE DEPARTMENT OF PHYSICS
NEHRU ARTS AND SCIENCE COLLEGE
KANHANGAD
KANNUR UNIVERSITY

CERTIFICATE

This is to certify that the project entitled "BIOMOLECULAR RECOGNITION OF SOME BIOACTIVE COMPOUNDS IN SPICES WITH AMYLOID-BETA PRECURSOR PROTEIN'' is the bonafide work done by KRISHNA SAGAR N Reg No. C1PSPH1603 PG Department of Physics, Nehru Arts and Science College Kanhangad, submitted to Kannur University for the partial fulfilment of the requirements for the award of DEGREE OF MASTER OF SCIENCE IN PHYSICS during the academic year 2021-2023.

Signature of Internal Guide

Dr. ATHIRA K M
HEAD OF THE DEPARTMENT (IN-CHARGE)
DEPARTMENT OF PHYSICS
NEHRU ARTS AND SCIENCE COLLEGE
KANHANGAD

Signature of External Guide

Dr. HARIS P
ASSISTANT PROFESSOR
DEPARTMENT OF PHYSICS
SIR SYED COLLEGE
TALIPARAMBA

Signature of External Examiners:

1.

2.

DECLARATION

I hereby declare that this project report entitled "BIOMOLECULAR RECOGNITION OF SOME BIOACTIVE COMPOUNDS IN SPICES WITH AMYLOID-BETA PRECURSOR PROTEIN" has been prepared by me in partial fulfilment of the MSc degree of Kannur University.I also assure that this project report has not been submitted by me fully or partially for the award of any degree before.

Nehru Arts And Science College
Kanhangad
June 2023

KRISHNA SAGAR N
Reg No: C1PSPH1603

ACKNOWLEDGMENT

I take this opportunity to express my sincere gratitude to all those who have been instrumental in the successful completion of this project.

Firstly, I thank Dr Haris P. Assistant Professor, PG Department of Physics, Sir Syed college, for all the help given to me for doing this project.

I thank Dr. Athira K M Hod-in charge, PG Department of Physics Nehru Arts and Science College, my internal guide for supporting me throughout to complete this project.

I deeply express my gratitude and appreciation to all teachers and lab staffs in physics department at Sir Syed College whose constant encouragement and valuable suggestion gave backbone in completing this work.

My sincere thanks to Principal Dr.K V Murali, Nehru Arts and Science College, Kanhangad for providing me the facilities needed to bring out this project.

A special thanks to all my friends for giving me confidence and strength to initiative this project.

Above all I thank God almighty. Without his blessing this effort would not have been a reality.

KRISHNA SAGAR N

TABLE OF CONTENTS

LIST OF TABLES

LIST OF FIGURES

LIST OF ABBREVIATIONS

- **DNA - Deoxyribonucleic acid**
- **RNA - Ribonucleic Acid**
- **AD - Alzheimer's Disease**
- **Aβ - β-Amyloid Peptide**
- **APP – Amyloid-Beta Precursor Protein**
- **TRPV1 - Transient Receptor Potential cation channel subfamily V member 1**
- **TRPA1 - Transient Receptor Potential cation channel subfamily A member 1**
- **NF-kb – Nuclear Factor kappa B**
- **MDMA - 3,4-Methylenedioxymethamphetamine**
- **MMDMA - 5-Methoxy-3,4-methylenedioxymethamphetamine**
- **ROS - Reactive Oxygen Species**
- **GNU - General Public License**
- **PDB - Protein Data Bank**
- **pdbqt – Protein Data Bank Q (partial charge) T (atom type)**
- **sdf – Space Delimited File/Format**
- **txt – Text**
- **jpf – Joint Photographic Experts Group**
- **gpf – Grid Parameter File**
- **dpf – Docking Parameter File**
- **glg – Grid Log File**
- **dlg – Docking Log File**
- **3-D – 3 Dimensional**
- **PubChem – Database of chemical molecule and their activities against biological assays**
- **CID – Compound Identifier**
- **MGL Tools – Molecular Graphics Laboratory Tools**
- **UCSF - University of California, San Francisco**
- **RMSD – Root Mean Square Deviation**

ABSTRACT

Alzheimer's disease is a progressive brain disorder characterized by the deposition of specific proteins, leading to detrimental changes in the brain over time. Among these proteins, Amyloid-beta precursor protein (APP) plays a crucial role. APP is an integral membrane protein expressed in various tissues and concentrated in neuronal synapses. It serves as a cell surface receptor and is involved in synaptic formation, neural plasticity, antimicrobial activity, and iron export. The gene APP codes for this protein, and its regulation is influenced by substrate presentation. Understanding the binding interactions between APP and various ligands is of great significance in drug design and pharmacology. This study focuses on investigating the binding interactions between Amyloid-beta precursor protein and bioactive compounds found in spices, employing molecular modeling and docking techniques using AUTODOCK software. The binding energies of the molecules involved were calculated, and APP complexes with favorable negative binding energies were identified. The findings of this study shed light on the potential bioactive compounds in spices that exhibit binding affinity towards Amyloid-beta precursor protein. These results have implications in the development of novel therapeutic interventions targeting Alzheimer's disease. Further exploration of the identified compounds may lead to the design and development of drugs that can modulate APP function and potentially mitigate the progression of Alzheimer's disease.

CHAPTER 1
INTRODUCTION

1.1 INTRODUCTION

Alzheimer's disease is a severe and widespread condition that impacts millions of people across the globe [1]. It is a degenerative brain disorder that leads to the gradual deterioration of memory and thinking capabilities, ultimately rendering Individuals incapable of performing basic daily activities. Despite dementia being more common among the elderly, Alzheimer's can afflict individuals of all ages [2]. The most significant risk factor for Alzheimer's is age, with the majority of patients being 65 years or older. Although no cure is available, several treatments are accessible that can temporarily slow the worsening of symptoms and enhance the quality of life of those with the disease and their caregivers. Two treatments that have demonstrated promise are Aducanumab and Lecanemab, which remove beta-amyloid from the brain and reduce cognitive and functional decline in early-stage Alzheimer's patients [3]. The primary symptom of Alzheimer's disease is memory loss, and early indications include difficulty recalling recent events or conversations. The disease progresses to cause more severe symptoms and declining cognitive function, with individuals becoming aware of their deteriorating memory and thinking capabilities [4]. It is crucial to recognize the early symptoms of Alzheimer's to provide the individual with proper medical attention and support. Alzheimer's disease is a serious condition that affects numerous individuals worldwide, and early detection and support are essential to enhance the quality of life of patients and their caregivers.

A biomolecule, also known as a biological molecule, is any of the many substances that are created by living things such as cells. Biomolecules come in a wide variety of shapes and sizes and carry out a wide range of tasks [5]. Proteins, lipids, nucleic acids, and carbohydrates are the four main categories of biomolecules. Nucleic acids, specifically DNA and RNA, are macromolecules with the special ability to store the genetic code of an organism. the nucleotide order that defines the proteins' amino acid composition, which is vital to life as we know it. A protein may contain any of the 20 distinct amino acids. Protein structure and function are

fundamentally influenced by the order in which they occur. Cells' primary structural constituents are proteins. They also operate as enzymes and catalysts for the vast majority of chemical events that take place in living creatures, transporting nutrients and other molecules into and out of cells. In addition to influencing gene activity, proteins also create hormones and antibodies. Protein structures can be categorised as primary, secondary, tertiary, or even quaternary [6]. These structures are based on the degree to which a polypeptide chain folds. Bioactive substances are a type of chemical that are present in plants and specific foods including fruits, vegetables, nuts, oils, and whole grains in very minute concentrations. Bioactive substances have physiological effects that could improve one's health [7]. Bioactive compounds in spices refer to the diverse group of naturally occurring chemical compounds that are present in spices and have a physiological effect on the human body. These compounds are typically present in small amounts but have been shown to have various health-promoting properties, such as antioxidant, anti-inflammatory, and anti-cancer activities [8].

Alzheimer's disease (AD) is the leading cause of dementia worldwide, characterized by the accumulation of the β-amyloid peptide (Aβ) within the brain along with hyperphosphorylated and cleaved forms of the microtubule-associated protein tau [9]. Amyloid-beta precursor protein is an ancient and highly conserved protein [10]. The amyloid beta precursor protein acts as a receptor on the surface of neurons and has important functions related to the growth and development of nerve cells, such as promoting neurite growth, helping neurons stick together, and aiding in the formation of axons. Synaptogenesis is promoted by the interaction of amyloid beta precursor protein (APP) molecules on adjacent cells [11].

Here I explored the mechanism and mode of interaction between Amyloid-beta precursor protein (APP) and some bioactive compounds in spices like Piperine, Cineole, Cinnamaldehyde, Eugenol, Zerumbone, Allicin, Myristicin, Curcumin using AutoDock 4.2.6 software.

1.2 AMYLOID-BETA PRECURSOR PROTEIN

Amyloid beta precursor protein (APP) is a type I transmembrane protein that is abundant in the nervous system, particularly in neurons. The gene APP is located on chromosome 21 in humans and contains 18 exons spanning 290 kilobases [12] [13]. Several alternative splicing isoforms of APP have been observed in humans, ranging in length from 639 to 770 amino acids, with certain isoforms preferentially expressed in neurons. Changes in the neuronal ratio of these isoforms have been associated with Alzheimer's disease [14]. APP is best known as the precursor molecule whose proteolysis generates amyloid beta (Aβ), a polypeptide containing 37 to 49 amino acid residues. The amyloid fibrillar form of Aβ is the primary component of amyloid plaques found in the brains of Alzheimer's disease patients. Mutations in critical regions of APP, including the region that generates Aβ, cause familial susceptibility to Alzheimer's disease [15] [16] [17] [18].

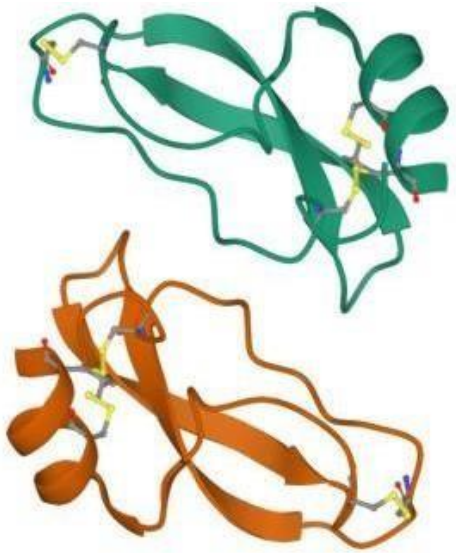

Figure 1.1 Crystal structure of Amyloid-beta precursor protein [19]

1.3 PIPERINE

Piperine is a natural alkaloid found in black pepper, long pepper, and other species of the Piperaceae family. It is responsible for the biting taste of black pepper [20]. Piperine is typically extracted from black pepper using organic solvents, such as dichloromethane, due to its low solubility in water [21]. The pain-sensing nerve cells, nociceptors, are activated by the heat and acidity-sensing channels TRPV1 and TRPA1, contributing to the pungency of piperine [22]. Piperine has been shown to have anti-inflammatory properties in various autoimmune diseases and cancer models [23]. Piperine has been found to affect cell signaling pathways, including the NF-kB pathway [24]. In various experimental situations of oxidative stress, piperine treatment has been shown to reduce lipid peroxidation and have a positive effect on anti-oxidant molecules and enzymes [25].

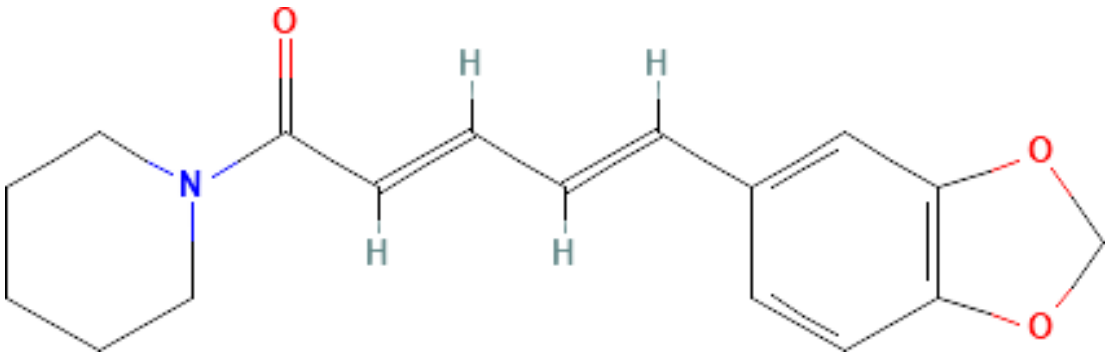

Figure 1.2 Structure of Piperine [26]

Formula: $C_{17}H_{19}NO_3$

Molar mass: 285.35 g/mol

1.4 CINEOLE

1,4-cineole is a natural organic compound found in various spices and herbs, where it contributes to their characteristic aroma and taste.1,4-Cineole belongs to the category of bicyclic epoxy monoterpenes, which are a group of chemical compounds. It is used as a flavouring [27] and can be obtained by reacting isoprene with sulfuric acid at 30°C [28] or through a stepwise reduction of ascaridole [29]. It is a colourless liquid with a camphor-like scent and is insoluble in water [27]. Along with its flavouring properties, 1,4-cineole is also known for its medicinal properties, such as reducing inflammation and alleviating respiratory symptoms. Although the concentration of 1,4-cineole in different spices can vary based on factors such as plant species, plant part used, and extraction method.

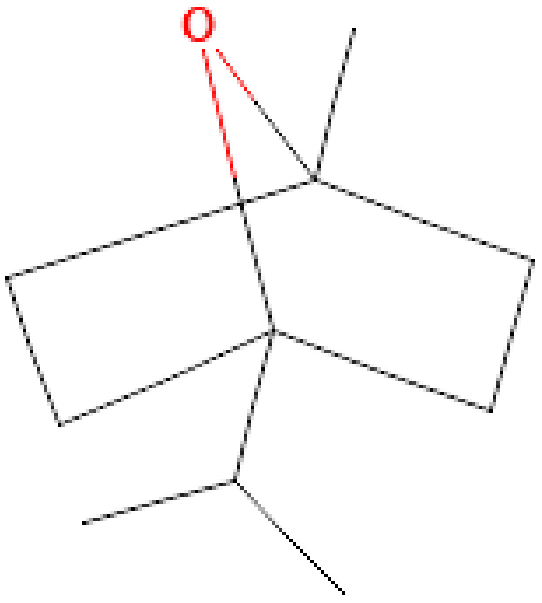

Figure 1.3 Structure of 1,4-Cineole [30]

Formula: $C_{10}H_{18}O$

Molar mass: 154.25 g/mol

1.5 CINNAMALDEHYDE

Cinnamon is a commonly used spice containing essential oils and derivatives, including cinnamaldehyde, cinnamic acid, and cinnamate [31]. Cinnamaldehyde is responsible for cinnamon's unique flavour and scent [32] and is naturally produced through the shikimate pathway [33]. It appears as a pale yellow, thick liquid found in the bark of cinnamon trees and other members of the Cinnamomum genus. The trans-cinnamaldehyde form is the natural variety and is a phenylpropanoid comprising an unsaturated aldehyde attached to a benzene ring. The molecule can be viewed as a derivative of acrolein. Cinnamaldehyde's colour is due to the increased $\pi \rightarrow \pi^*$ transition, which is a result of its greater conjugation than acrolein [34]. Cinnamaldehyde can be utilized to deceive people by adding it to powdered beechnut husk and selling it as powdered cinnamon [35]. Cinnamaldehyde has the ability to inhibit corrosion in steel and other alloys, as it is thought to create a protective layer on the surface of the metal. [36].

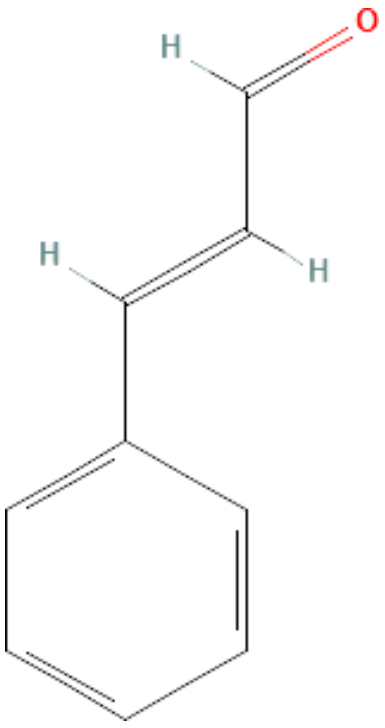

Figure 1.4 Structure of Cinnamaldehyde [37]

Formula: C_9H_8O

Molar mass: 132.16 g/mol

1.6 EUGENOL

Eugenol is a member of the allylbenzene class of chemical compounds, and it is an allyl chain-substituted guaiacol [38]. It is extracted from certain essential oils, particularly from clove, nutmeg, cinnamon, basil, and bay leaf, and is a colourless to pale yellow, aromatic oily liquid [39] [40] [41] [42]. Eugenol has a pleasant, spicy, clove-like scent [43] and is used as a flavour or aroma ingredient in teas, meats, cakes, perfumes, cosmetics, flavourings, and essential oils [38]. It is also used as a local antiseptic and anesthetic [44] [45]. In addition to its use in consumer products, eugenol also has a range of potential medicinal benefits. For example, it has anti-inflammatory and analgesic properties, and may help to relieve pain associated with conditions such as toothache and arthritis. It also has antimicrobial properties, and may be effective against certain strains of bacteria and fungi [38]. However, eugenol can also be harmful if ingested in high doses for extended periods of time. It may cause liver toxicity [46], and has been shown to have mutagenic and carcinogenic effects in some studies.

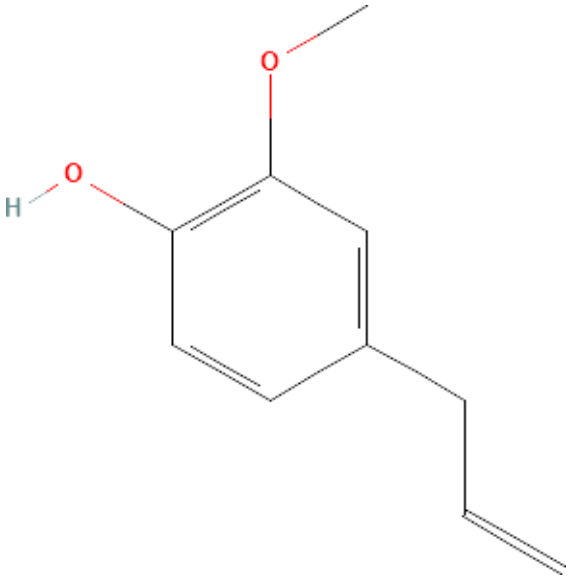

Figure 1.5 Structure of Eugenol [47]

Formula: $C_{10}H_{12}O_2$

Molar mass: 164.2 g/mol

1.7 ZERUMBONE

Zerumbone is a highly volatile monocyclic sesquiterpene compound found in large amounts in the rhizome of wild edible ginger, Zingiber zerumbet (L.) Roscoe ex Sm. essential oil [48,49]. This rhizomatous herbaceous species, belonging to the Zingiberaceae family, is also known as bitter ginger, shampoo ginger, and pinecone ginger. It has applications as a flavouring and appetizing agent and for treating pain in folk medicine [50,51]. Zerumbone exhibits various biological activities, such as antimicrobial, antioxidant, anti-inflammatory, antitumor, or antihyperalgesic, attributed to the structure of this bioactive compound biosynthesized from α-humulene [52]. It exhibits significant cytotoxic activity against lung, colon, leukemia, ovarian, skin, liver, and breast cancers, with selective cytotoxic activity on human tumour cell lines, not found with the structural analogue, α-humulene, that lacks the carbonyl group [51,53,54,55,56]. Furthermore, zerumbone has been shown to have potential as a therapeutic agent for various diseases, including Alzheimer's disease, rheumatoid arthritis, and diabetes, due to its anti-inflammatory and antioxidant properties [57,58,59]. Additionally, it has been found to have hepatoprotective effects and to be effective in the treatment of liver fibrosis [60,52].

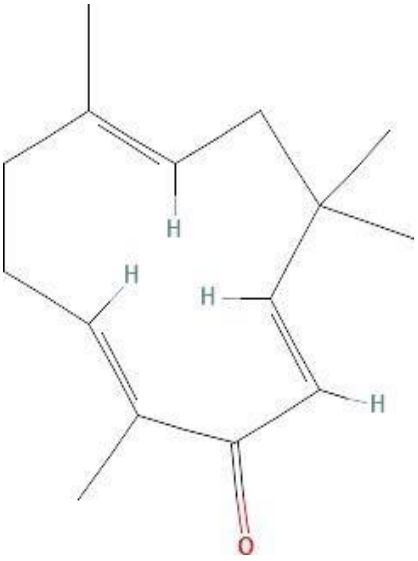

Figure 1.6 Structure of Zerumbone [61]

Formula: $C_{15}H_{22}O$

Molar mass: 218.33 g/mol

1.8 ALLICIN

Allicin is an organosulfur compound obtained from garlic, a species in the family Alliaceae [62]. When fresh garlic is chopped or crushed, the enzyme alliinase converts alliin into allicin, which is responsible for the aroma of fresh garlic [63]. Allicin is an oily, slightly yellow liquid that gives garlic its distinctive odour. It is a thioester of sulfenic acid and is also known as allyl thiosulfinate [64]. Produced in garlic cells, allicin is released upon disruption, producing a potent aroma when garlic is cut or cooked, and is among the chemicals responsible for both the smell and flavour of garlic [65][66]. The allicin generated is unstable and quickly changes into a series of other sulfur-containing compounds such as diallyl disulfide [65]. Allicin is part of a defence mechanism against attacks by pests on the garlic plant [66]. Its biological activity can be attributed to both its antioxidant activity and its reaction with thiol-containing proteins [67]. Allicin has a range of biological activities, including antibacterial, antifungal, and antiparasitic effects.

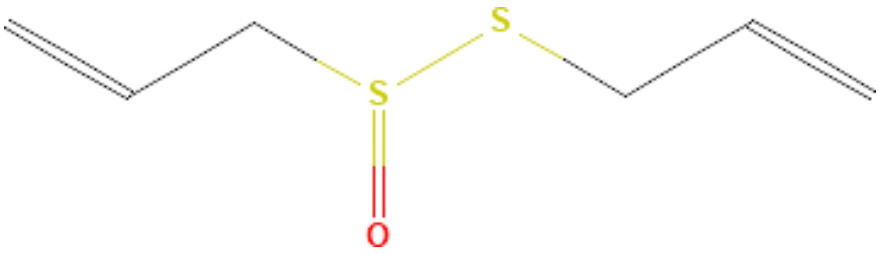

Figure 1.7 Structure of Allicin [68]

Formula: $C_6H_{10}OS_2$

Molar mass: 162.3 g/mol

1.9 MYRISTICIN

Myristicin is a naturally occurring substance present in various herbs and spices, including nutmeg. It is also found in black pepper and several members of the Umbelliferae family, such as anise, carrots, parsley, celery, dill [69], and parsnip [70]. The use of isolated myristicin has shown effectiveness as an insecticide against several pests that commonly affect agriculture [71]. Myristicin has a chemical structure that is similar to amphetamine compounds, and it can produce psychotropic effects similar to MDMA (3,4-methyl anedioxy methamphetamine) compounds. As a result, it is possible to use myristicin in the creation of amphetamine derivatives and designer drugs, such as MMDMA (5-Methoxy-3,4-methylenedioxymethamphetamine) that have comparable chemical structures and effects to MDMA [72]. Ingesting myristicin may lead to hallucinogenic effects [73], and it has the potential to be converted into MMDMA through controlled chemical synthesis [72]. Myristicin interacts with multiple enzymes and signaling pathways within the body [74] [75]and could have cytotoxic effects on living cells, with the degree of cytotoxicity varying with the dosage [74]. According to research, myristicin has various properties that are beneficial for the human body, including anti-inflammatory and antioxidant properties. It also exhibits antimicrobial properties that can help combat pathogenic bacteria and fungi, acts as an insecticide and larvicide, and has antiproliferative activity that can be useful against several types of cancer cells [76].

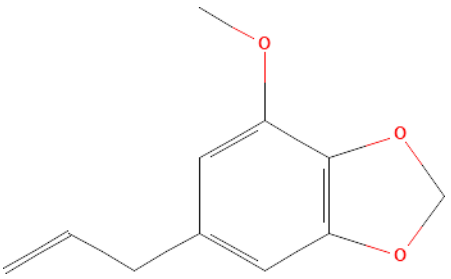

Figure1.8 Structure of Myristicin [77]

Formula: $C_{11}H_{12}O_3$

Molar mass: 192.21 g/mol

1.10 CURCUMIN

Curcumin, a bright yellow chemical, is derived from Curcuma longa plants and is the primary curcuminoid found in turmeric. Turmeric belongs to the ginger family known as Zingiberaceae. Curcumin is marketed as a food flavoring, food coloring, herbal supplement, and cosmetic ingredient [78]. Curcumin is a yellow-orange solid with a molecular weight of 368 g/mol and a melting point of 183 °C. It is a polyphenolic compound consisting of two aromatic rings, each with one hydroxy and one methoxy substituent. The two rings are linked by a seven-carbon chain that contains two α-β unsaturated carbonyl groups, which can undergo tautomerization [79]. Curcumin possesses remarkable antioxidant properties by binding to iron, preventing lipid peroxidation, and scavenging reactive oxygen species (ROS) [80]. It also exhibits anti-inflammatory properties in both acute and chronic inflammation [81]. Besides these effects, curcumin is being extensively investigated for its potential to serve as an anticancer agent [82]. Curcumin is present in various spices and food items and can be consumed in relatively high quantities as a part of daily diets without any adverse side effects. Therefore, it has the potential to serve as a promising chemopreventive or therapeutic agent [83].

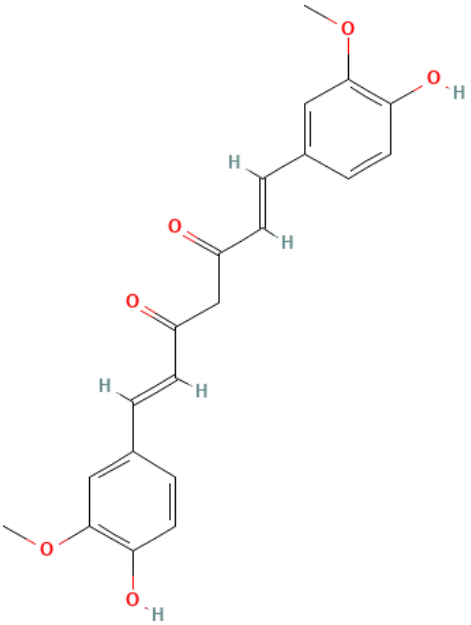

Figure 1.9 Structure of Curcumin [84]

Formula: $C_{21}H_{20}O_6$

Molar mass: 368.4 g/mol

1.11 AUTODOCK

Autodock is a molecular modeling stimulation software [85]. It is especially effective for protein ligand docking. Autodock4.2 is available under the GNU general public License. Autodock is one of the most cited docking software applications in the research community. It is designed to predict how small molecules, such as substrares or drug candidates, bind to a receptor of known 3D structure. Autodock has application in X-ray crystallography, structure based drug design, virtual screening, protein-protein docking, chemical mechanism studies etc [86].

AutoDock 4.2.6 is a software package used for molecular docking simulations, which are computational methods that predict the binding mode and binding affinity of small molecules, such as drugs, to larger macromolecules, such as proteins or nucleic acids. The AutoDock 4.2.6 software uses a search algorithm to explore the conformational space of a small molecule ligand within the binding site of a macromolecule, in order to find the optimal binding pose. The search algorithm uses a combination of random search and local optimization techniques to sample the conformational space efficiently. The software also includes an energy scoring function to evaluate the fitness of each ligand conformation. The scoring function is based on the Lamarckian Genetic Algorithm, which is an optimization algorithm that uses a population-based approach to find the best docking pose. The AutoDock 4.2.6 software uses a force field to calculate the energy of each ligand conformation. A force field is a mathematical model that describes the interactions between atoms and molecules, and it is used to calculate the potential energy of a molecular system. In AutoDock 4.2.6, the force field is used to calculate the van der Waals and electrostatic interactions between the ligand and the macromolecule, as well as the desolvation energy of the ligand. The force field used in AutoDock 4.2.6 is a modified version of the Amber force field. The modifications were made to improve the accuracy of the force field for protein-ligand interactions. The force field parameters were derived from quantum mechanical calculations and experimental data [87] [88].

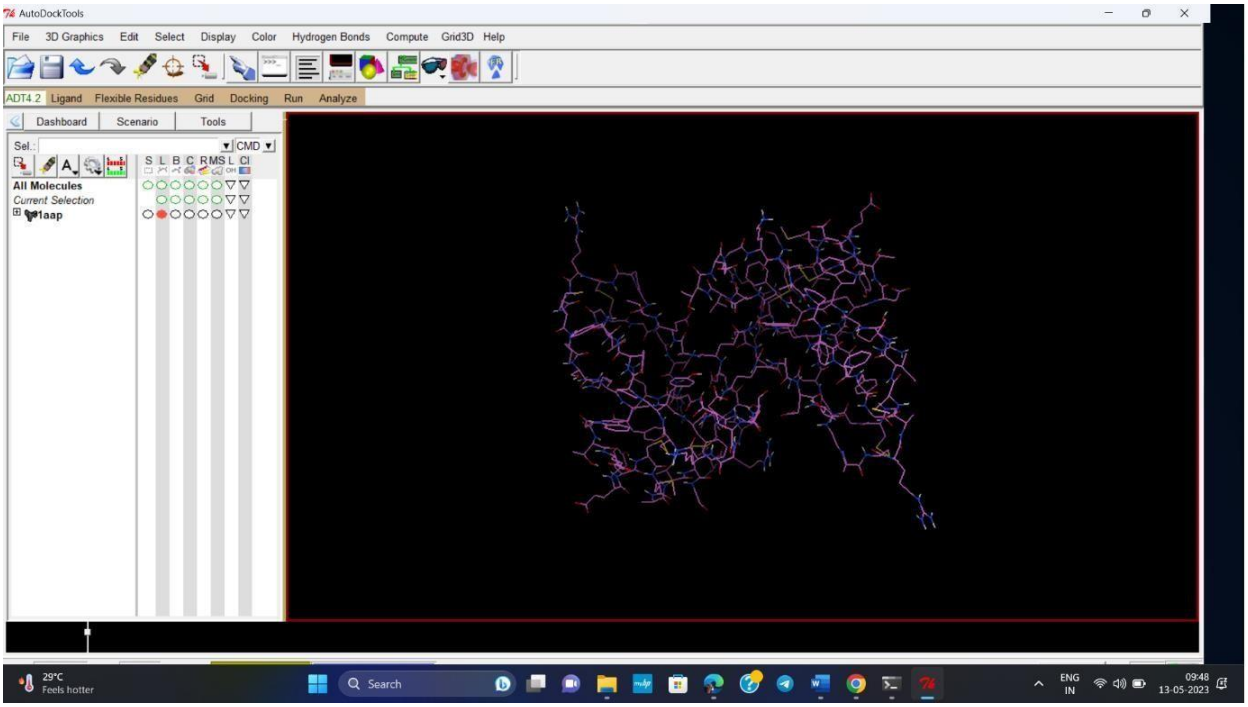

Figure 1.10 AutoDock Window

CHAPTER 2

MATERIALS AND METHODS

2.1 MATERIALS

2.1.1 AUTODOCK

The molecular docking studies were performed to explore the interactions between some bioactive compounds in spices and Amyloid-beta precursor protein (APP) by using AutoDock program version 4.2.6.

2.1.2 AMYLOID-BETA PRECURSOR PROTEIN (APP)

The 3-D dimensional crystal structure of Amyloid-beta precursor protein (APP-PDB ID 1AAP) [19] was taken from the protein data bank (PDB). PDB is a database for the 3D structural data of large biological molecules, such as protein nuclei acids [89]. The data is typically obtained by X ray crystallography, NMR spectroscopy etc. (https://www.rcsb.org/pdb).

2.1.3. LIGANDS

The 3D structure of ligands downloaded from PubChem data basis. It is database of chemical molecules and their activities against biological assays (https://pubchem.ncbi.nlm.nih.gov).

- Piperine - PubChem CID: 638024
- 1,4 Cineole - PubChem CID: 10106
- Cinnamaldehyde - PubChem CID: 637511
- Eugenol - PubChem CID: 3314
- Zerumbone - PubChem CID: 5470187
- Allicin - PubChem CID: 65036
- Myristicin - PubChem CID: 4276
- Curcumin – PubChem CID: 969516

2.2 METHODS

Below are the steps followed for the molecular docking analysis of the above-mentioned bioactive compounds (ligands) with the protein Amyloid-beta Precursor Protein:

1. Download and install the following software:

- AutoDock 4.2.6
- MGL Tools
- UCSF Chimera

2. Download the crystal structure of the Amyloid-beta Precursor Protein from the Protein Data Bank (PDB) in PDB format.
3. Download the ligands from PubChem in SDF format.
4. Convert the ligands from SDF format to PDB format using UCSF Chimera.
5. Create a folder and copy the selected protein and ligands (both in PDB format) into that folder.
6. Open AutoDock and go to "File" -> "Preferences" -> Add the folder name -> Make it the default folder -> Set.
7. Load the protein by going to "File" -> "Read Molecule" -> Select the protein in PDB format.
8. Remove water molecules by going to "Edit" -> "Delete Water".
9. Add hydrogen atoms by going to "Edit" -> "Hydrogen" -> Select "Polar only".
10. Assign charges to the molecule by going to "Edit" -> "Charge".
11. Save the modified protein structure in PDB format by going to "File" -> "Save" -> Write PDB.
12. Load the ligand by going to "Ligand" -> "Input" -> Open -> Select the ligand in PDB format.
13. Define the torsion tree by going to "Ligand" -> "Torsion Tree" -> Choose the root -> Detect the root -> Choose torsion -> Set the number of torsions.
14. Save the modified ligand structure in PDBQT format by going to "Ligand" -> "Output" -> Save PDBQT.

Set up the grid parameters by going to "Grid" -> "Macromolecule" -> Choose ->

1. Select the protein (filename.pdbqt).
2. Set the map type to "Ligand" and select the ligand (name of selected ligand).
3. Define the grid box by going to "Grid" -> "Grid Box" -> We can choose normal or blind docking depending on our requirements. Here I chose blind docking. In blind docking, we extend the docking box to cover the entire protein structure, allowing the ligand to explore various potential binding sites within the protein.
4. Close the current file by going to "File" -> "Close Saving Current".
5. Save the grid dimensions in a text file by going to "Grid" -> "Grid Box" -> "File" -> "Output Grid Dimensional File" -> Save as filename.txt.
6. Save the grid parameter file (GPF) by going to "Grid" -> "Output" -> "SaveGPF" -> Save as filename.gpf.
7. Edit the GPF file as needed and click "OK".
8. Set up the docking parameters by going to "Docking" -> "Macromolecule" -> "Set Rigid Filename" -> Select the filename as saved in the grid (filename.pdbqt).
9. Select the ligand for docking by going to "Docking" -> "Ligand" -> "Choose" -> Select the ligand -> Accept.
10. Set the search parameters by going to "Docking" -> "Search Parameters" -> Choose the Genetic Algorithm -> Accept.
11. Set the docking parameters by going to "Docking" -> "Docking Parameters" -> Accept.
12. Save the docking parameter file (DPF) by going to "Docking" -> "Output" -> "Lamarckian" -> Save as filename.dpf.
13. Edit the DPF file as needed and click "OK".
14. Run the AutoGrid program by going to "Run" -> "AutoGrid" -> "Program Pathname" -> Browse -> Select the path where AutoGrid is located -> Open.
15. Set the parameter file name by browsing and selecting the previously saved GPF file.
16. The log filename will be filled automatically in GLG format.
17. Click "Launch" and wait for the process to complete.
18. Run the AutoDock program by going to "Run" -> "AutoDock" -> "Program Pathname" -> Browse -> Select the path where AutoDock is located -> Open.
19. Set the parameter file name by browsing and selecting the previously saved DPF file.
20. The log filename will be filled automatically in DLG format.

15. Click "Launch" and wait for the process to complete.
16. Analyze the results by going to "Analyse" -> "Docking" -> "Open" -> Select the DLG file -> Open -> OK.
17. The 3D figure of the ligand will be displayed.

After completing the docking process using AutoDock, you can further analyze the results using AutoDock Tools with the following steps:

1. Analyze the docking interactions by going to "Analyse" -> "Docking" -> "Show Interaction". This will display an interaction picture showing the interactions between the ligand and protein. You can adjust the background color to enhance the visibility of the interactions.
2. Load and analyze different conformations by going to "Analyse" -> "Conformation" -> "Load".
3. Play the docking trajectory by going to "Analyse" -> "Play".
4. Save an image of the docking result by going to "Save Image" and selecting the output file format, such as .jpg or .png. Click "OK" to save the image.
5. Analyze the clustering of docking results by going to "Analyse" -> "Clustering" -> "Show". This will display a graph showing the binding energy versus conformations in the angstrom of the ligand with the protein. The clustering analysis helps identify the best conformation with the lowest binding energy.

Hence by utilizing AutoDock Tools, I could visualize, analyze, and interpret the docking results to gain insights into the ligand-protein interactions and select the most favorable docking conformations based on the binding energy.

CHAPTER 3

RESULT AND ANALYSIS

The mode of binding and affinity of APP with small molecules were analyzed using Autodock software.

3.1 BINDING ANALYSIS

3.1.1 PIPERINE WITH APP

The biomolecular recognition of Piperine with APP was studied by Molecular Docking using AutoDock software. According to the results, the binding process between Piperine and APP is primarily governed by hydrophobic interactions and hydrogen bond forces. Out of the 10 obtained docking conformations, the conformation with lowest free binding energy was selected and analyzed. The lowest binding energy is obtained for the 6^{th} conformations. The lowest binding energy in this Piperine-APP interaction is -5.77 kcal/mol. As shown in Figure 3.1 Piperine inserted into the APP with a free binding energy of -5.77kcal/mol.

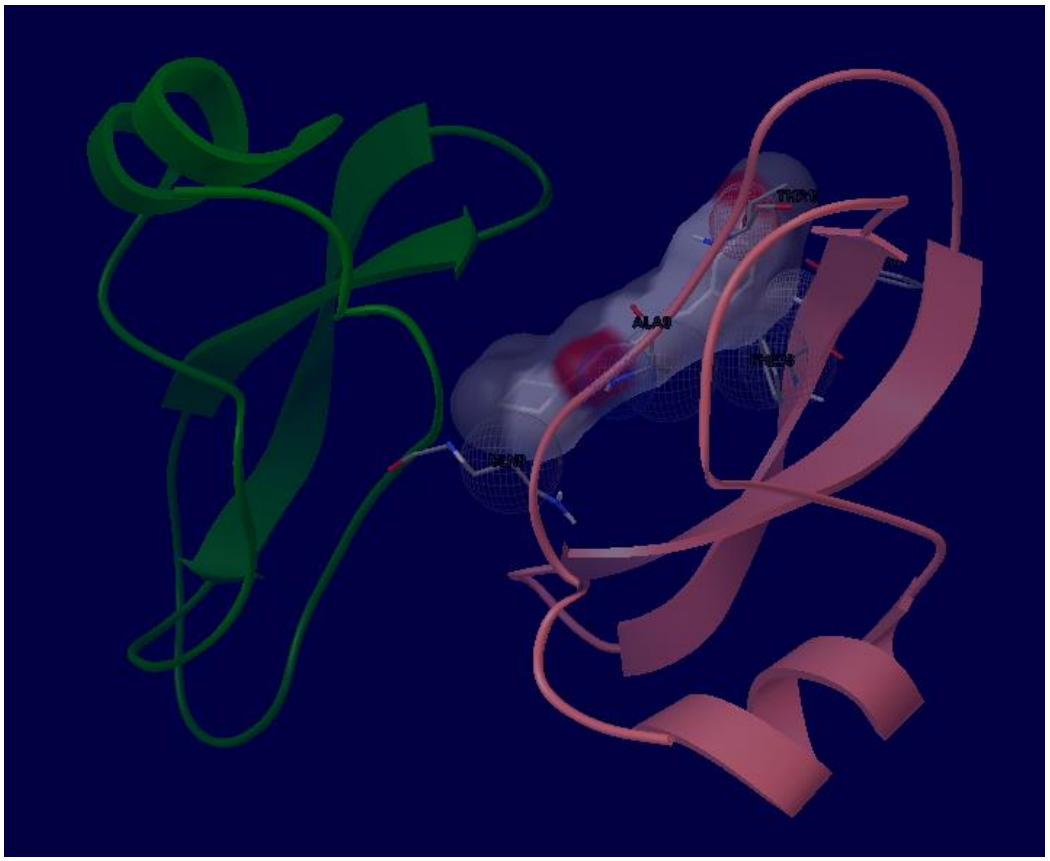

Figure 3.1 Interaction of Piperine with APP

Figure 3.2 Illustrates the details of the binding forces of Piperine with the surrounding amino acids residues. GLY39, ARG42, VAL3, VAL1 are the various amino acids residues that bind with ligand (Piperine) molecule.

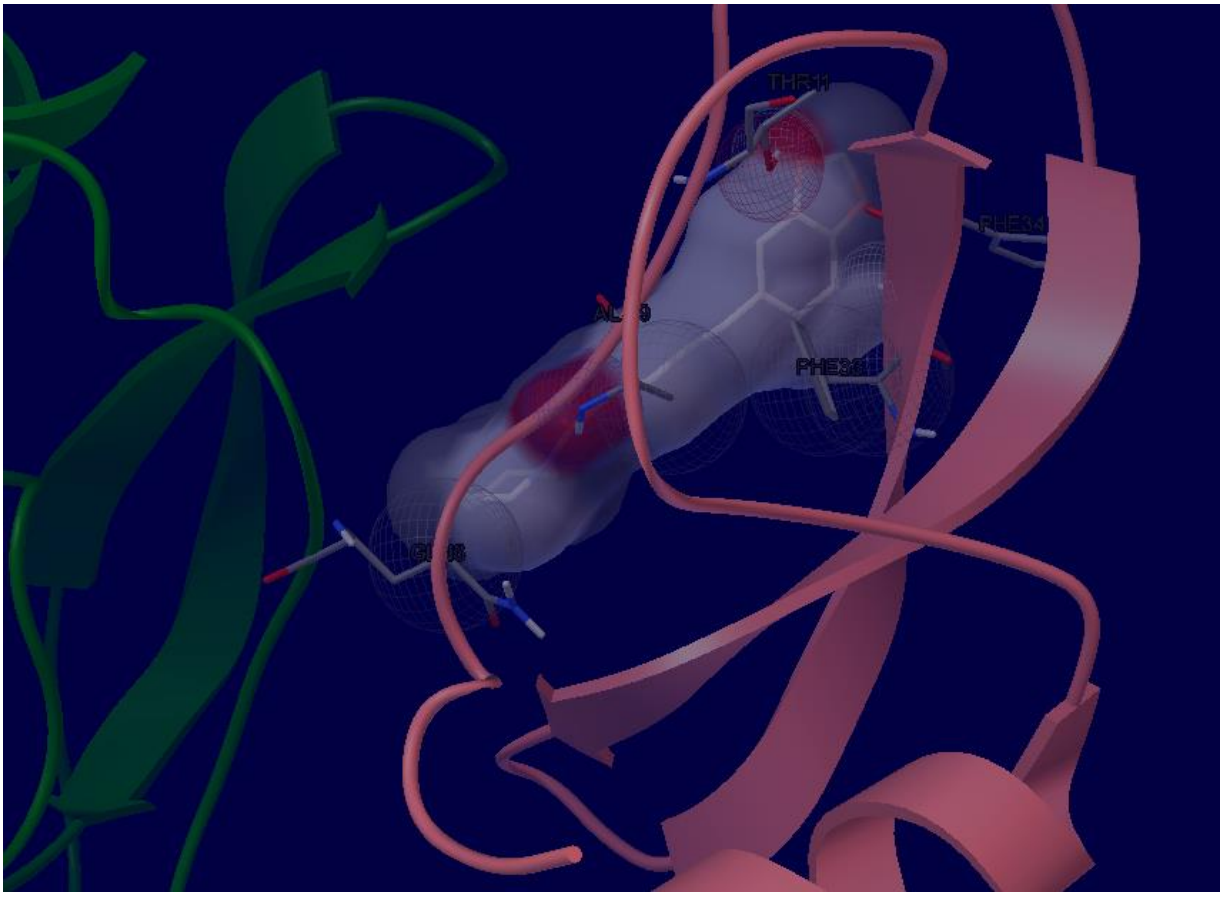

Figure 3.2 Detailed illustration of the binding forces of Piperine with the surrounding amino acid residues of APP.

The Figure 3.3 illustrates a representative example of the clustering analysis conducted on the docked poses for Piperine with APP. The root mean square deviation (RMSD) from the reference structure is found to be 39.63 Å. Here we used rmsd-tolerance of 2 Å. The estimated inhibition constant (Ki) for this interaction is determined to be 58.60 uM (micromolar) at a temperature of 298.15 K.

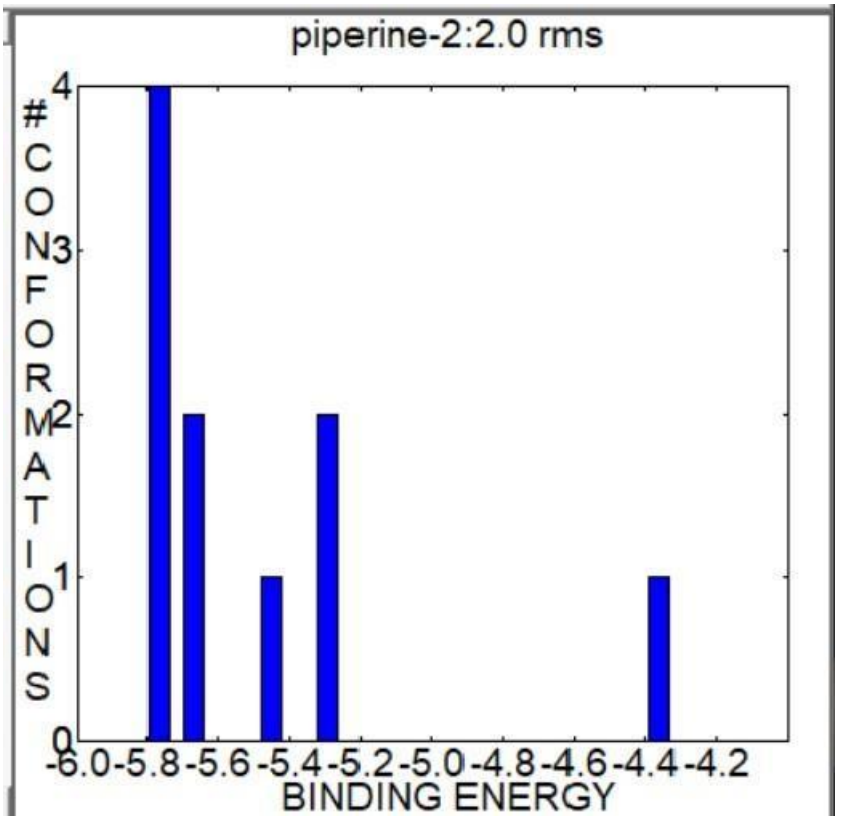

Figure 3.3 A graph representing the binding energy versus conformations in the angstrom units of Piperine with APP.

The statistical mechanical calculations were done for the binding process of Piperine with APP and tabulated as shown in Table 3.1. The partition function, free energy, internal energy, entropy, and binding energy of the interaction were given in the table. The binding process between Piperine and APP was spontaneous and entropy driven.

Receptor	**Ligand**	**Partition function (Q) Kcal/mol**	**Free energy (A) Kcal/mol**	**Internal energy (U) Kcal/mol**	**Entropy (S) Kcal/mol/K**	**Binding energy Kcal/mol**
APP	Piperine	10.09	-1369.67	-5.43	4.58	-5.77

Table 3.1 The statistical mechanical analysis results of Piperine with APP

3.1.2 CINEOLE WITH APP

The biomolecular recognition of Cineole with APP was studied by Molecular Docking using AutoDock software. According to the results, the binding process between Cineole and APP is primarily governed by hydrophobic interactions and hydrogen bond forces. Out of the 10 obtained docking conformations, the conformation with lowest free binding energy was selected and analyzed. The lowest binding energy is obtained for the 3rd conformations. The lowest binding energy in this Cineole-APP interaction is -4.41kcal/mol. As shown in Figure 3.4 Cineole inserted into the APP with a free binding energy of -4.41 kcal/mol.

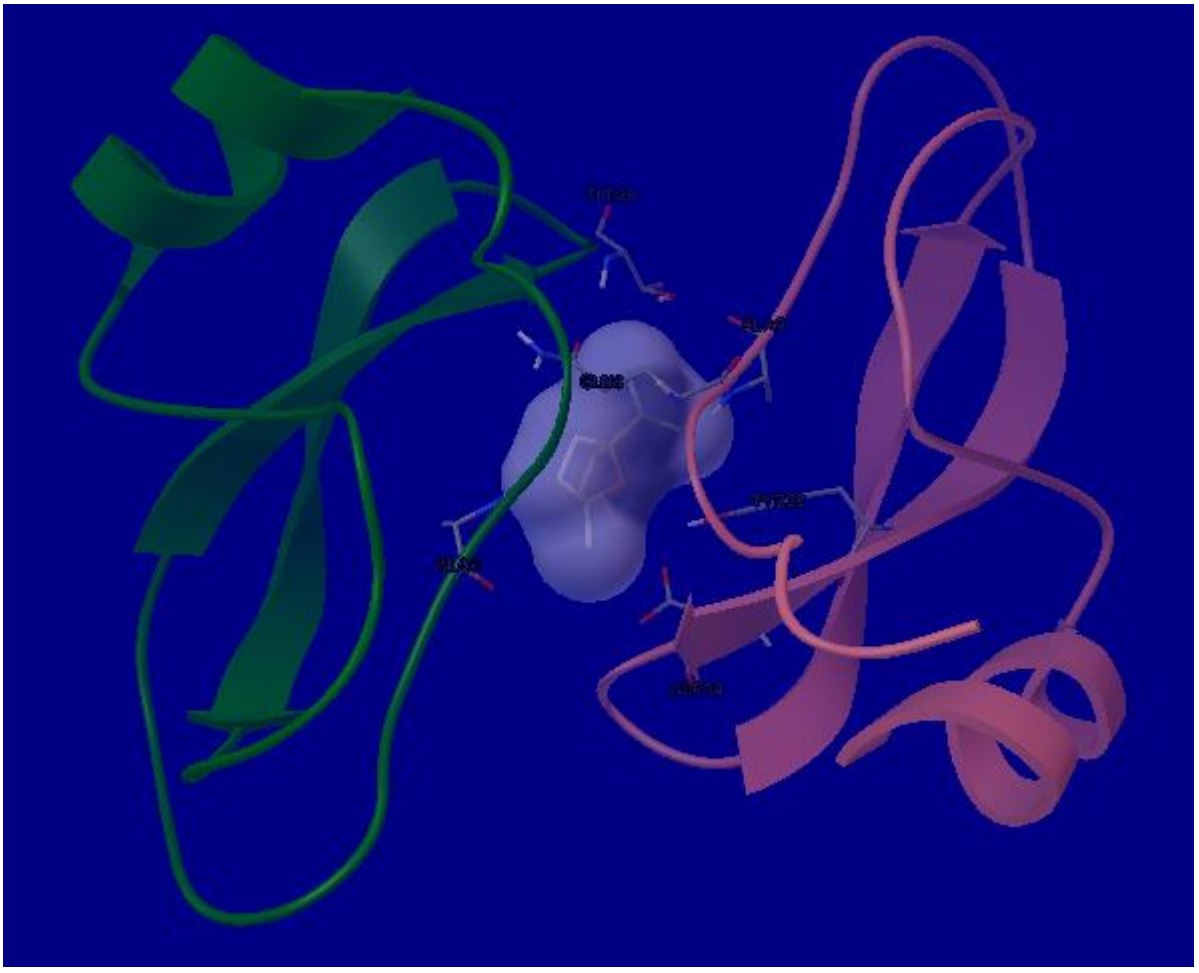

Figure 3.4 Interaction of Cineole with APP

Figure 3.5 Illustrates the details of the binding forces of Cineole with the surrounding amino acids residues. THR26, GLN8, ALA9, TYR22, ASP24 are the various amino acid residues that bind with ligand (Cineole) molecule.

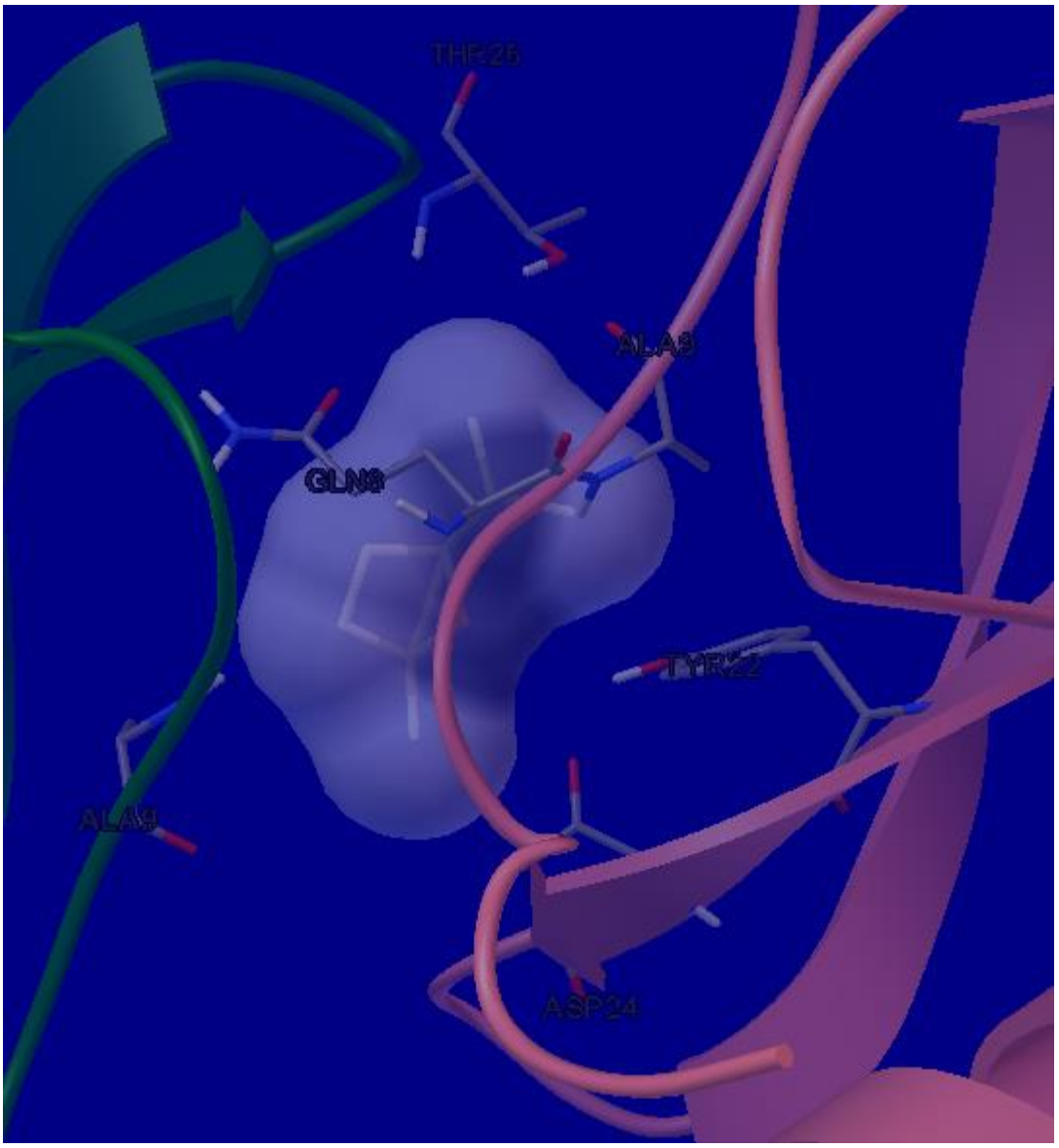

Figure 3.5 Detailed illustration of the binding forces of Cineole with the surrounding amino acid residues of APP.

The Figure 3.6 illustrates a representative example of the clustering analysis conducted on the docked poses for Cineole binding to APP. The root mean square deviation (RMSD) from the reference structure is found to be 41.83 Å. Here we used RMSD tolerance of 2 Å. The estimated inhibition constant (Ki) for this interaction is determined to be 589.60 uM (micromolar) at a temperature of 298.15 K.

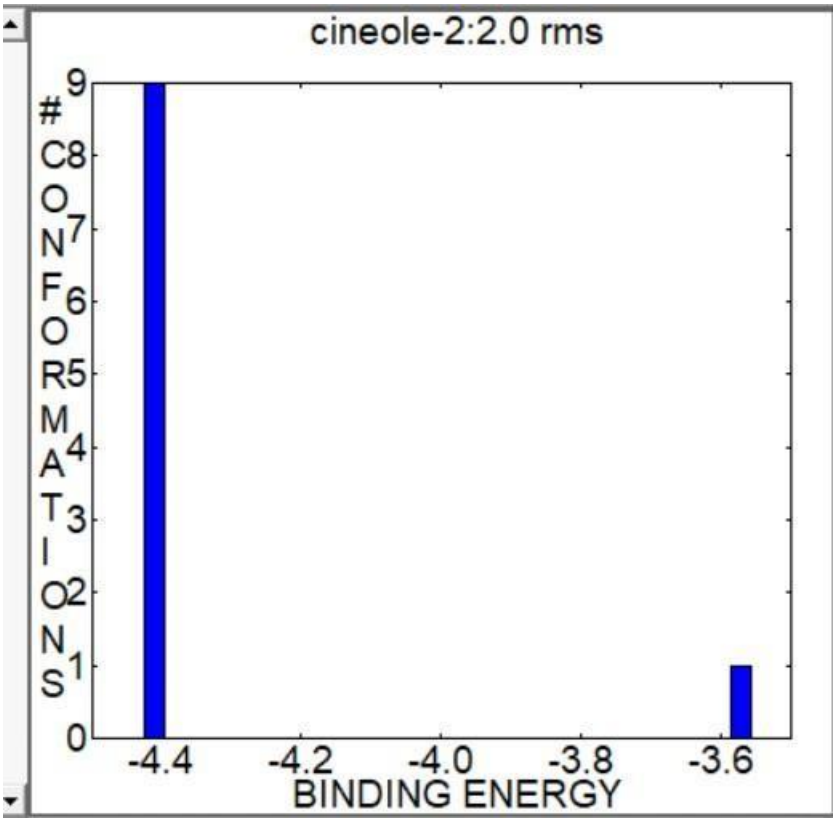

Figure 3.6 A graph representing the binding energy versus conformations in the angstrom units of Cineole with APP.

The statistical mechanical calculations were done for the binding process of Cineole with APP and tabulated as shown in Table 3.2. The partition function, free energy, internal energy, entropy, and binding energy of the interaction were given in the table. The binding process between Cineole and APP was spontaneous and entropy driven.

Receptor	**Ligand**	**Partition function (Q) Kcal/mol**	**Free energy (A) Kcal/mol**	**Internal energy (U) Kcal/mol**	**Entropy (S) Kcal/mol/K**	**Binding energy Kcal/mol**
APP	Cineole	10.07	-1368.43	-4.19	4.58	-4.41

Table 3.2 The statistical mechanical analysis results of Cineole with APP

3.1.3 CINNAMALDEHYDE WITH APP

The biomolecular recognition of Cinnamaldehyde with APP was studied by Molecular Docking using AutoDock software. According to the results, the binding process between Cinnamaldehyde and APP is primarily governed by hydrophobic interactions and hydrogen bond forces. Out of the 10 obtained docking conformations, the conformation with lowest free binding energy was selected and analyzed. The lowest binding energy is obtained for the 3rd conformations. The lowest binding energy in this Cinnamaldehyde-APP interaction is -3.96 kcal/mol. As shown in Figure 3.7 Cinnamaldehyde inserted into the APP with a free binding energy of -3.96 kcal/mol.

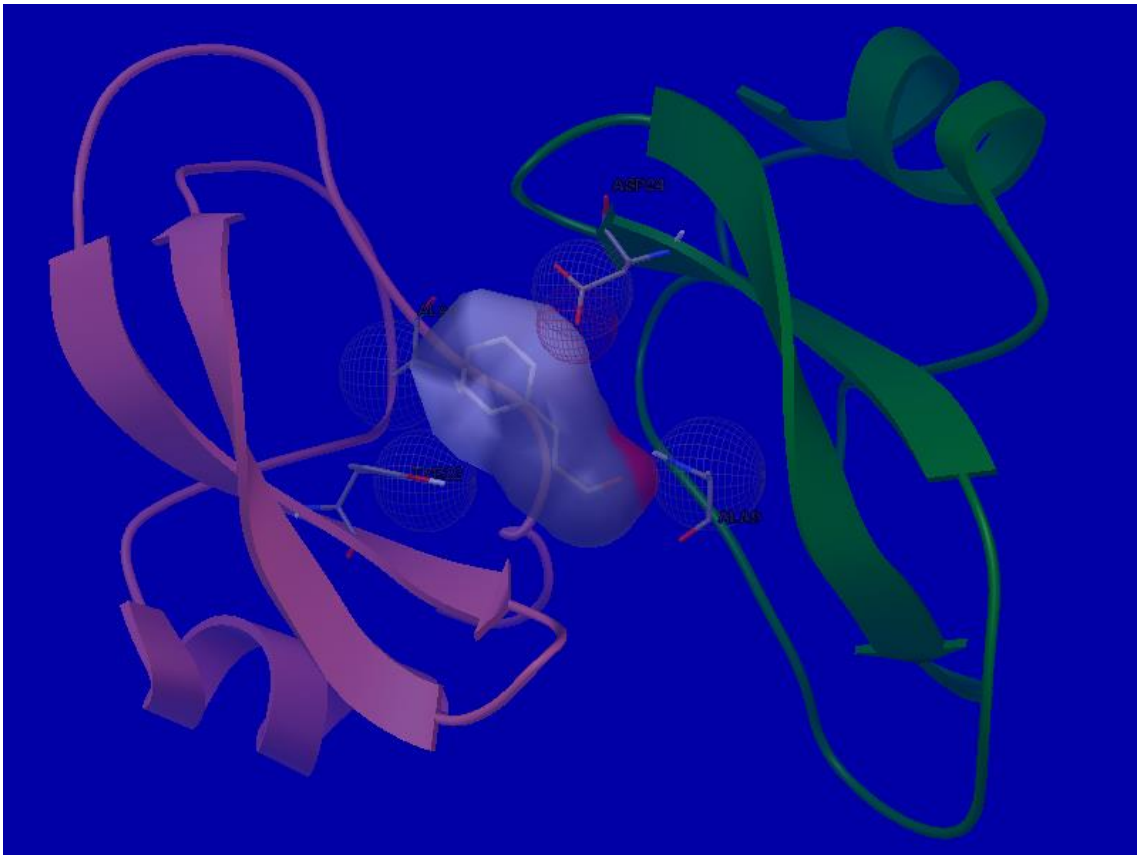

Figure 3.7 Interaction of Cinnamaldehyde with APP

Figure 3.8 Illustrates the details of the binding forces of Cinnamaldehyde with the surrounding amino acid residues. ASP24, ALA9, TYR22 are the various amino acid residues that bind with the ligand (Cinnamaldehyde) molecule.

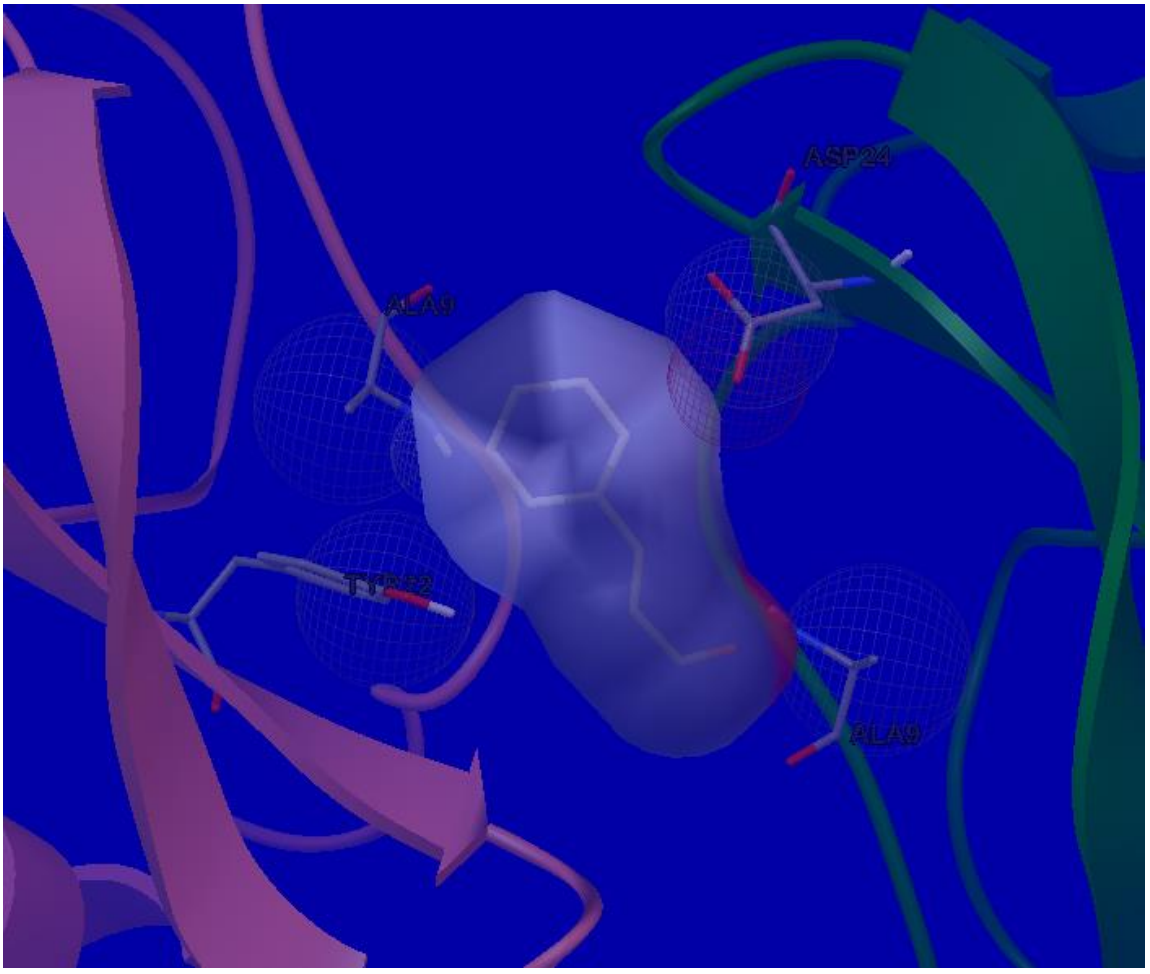

Figure 3.8 Detailed illustration of the binding forces of Cinnamaldehyde with the surrounding amino acid residues of APP.

The Figure 3.9 illustrates a representative example of the clustering analysis conducted on the docked poses for Cinnamaldehyde binding to APP. The root mean square deviation (RMSD) from the reference structure is found to be 42.53 Å. Here we used RMSD tolerance of 2 Å. The estimated inhibition constant (Ki) for this interaction is determined to be 1.01 mM (millimolar) at a temperature of 298.15 K.

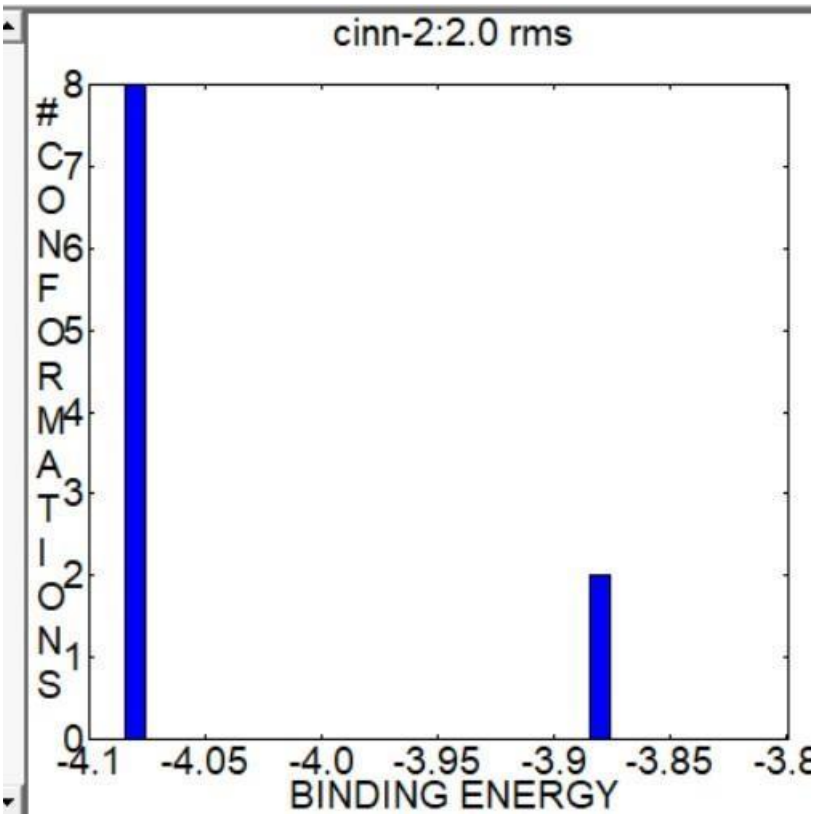

Figure 3.9 A graph representing the binding energy versus conformations in the angstrom units of Cinnamaldehyde with APP.

The statistical mechanical calculations were done for the binding process of Cinnamaldehyde with APP and tabulated as shown in Table 3.3. The partition function, free energy, internal energy, entropy, and binding energy of the interaction were given in the table. The binding process between Cinnamaldehyde and APP was spontaneous and entropy driven.

Receptor	**Ligand**	**Partition function (Q) Kcal/mol**	**Free energy (A) Kcal/mol**	**Internal energy (U) Kcal/mol**	**Entropy (S) Kcal/mol/K**	**Binding energy Kcal/mol**
APP	Cinnamaldehyde	10.07	-1368.17	-3.93	4.58	-3.96

Table 3.3 The statistical mechanical analysis results of Cinnamaldehyde with APP

3.1.4 EUGENOL WITH APP

The biomolecular recognition of Eugenol with APP was studied by Molecular Docking using AutoDock software. According to the results, the binding process between Eugenol and APP is primarily governed by hydrophobic interactions and hydrogen bond forces. Out of the 10 obtained docking conformations, the conformation with lowest free binding energy was selected and analyzed. The lowest binding energy is obtained for the 2nd conformations. The lowest binding energy in this Eugenol-APP interaction is -3.37 kcal/mol. As shown in Figure 3.10 Eugenol inserted into the APP with a free binding energy of -3.37kcal/mol.

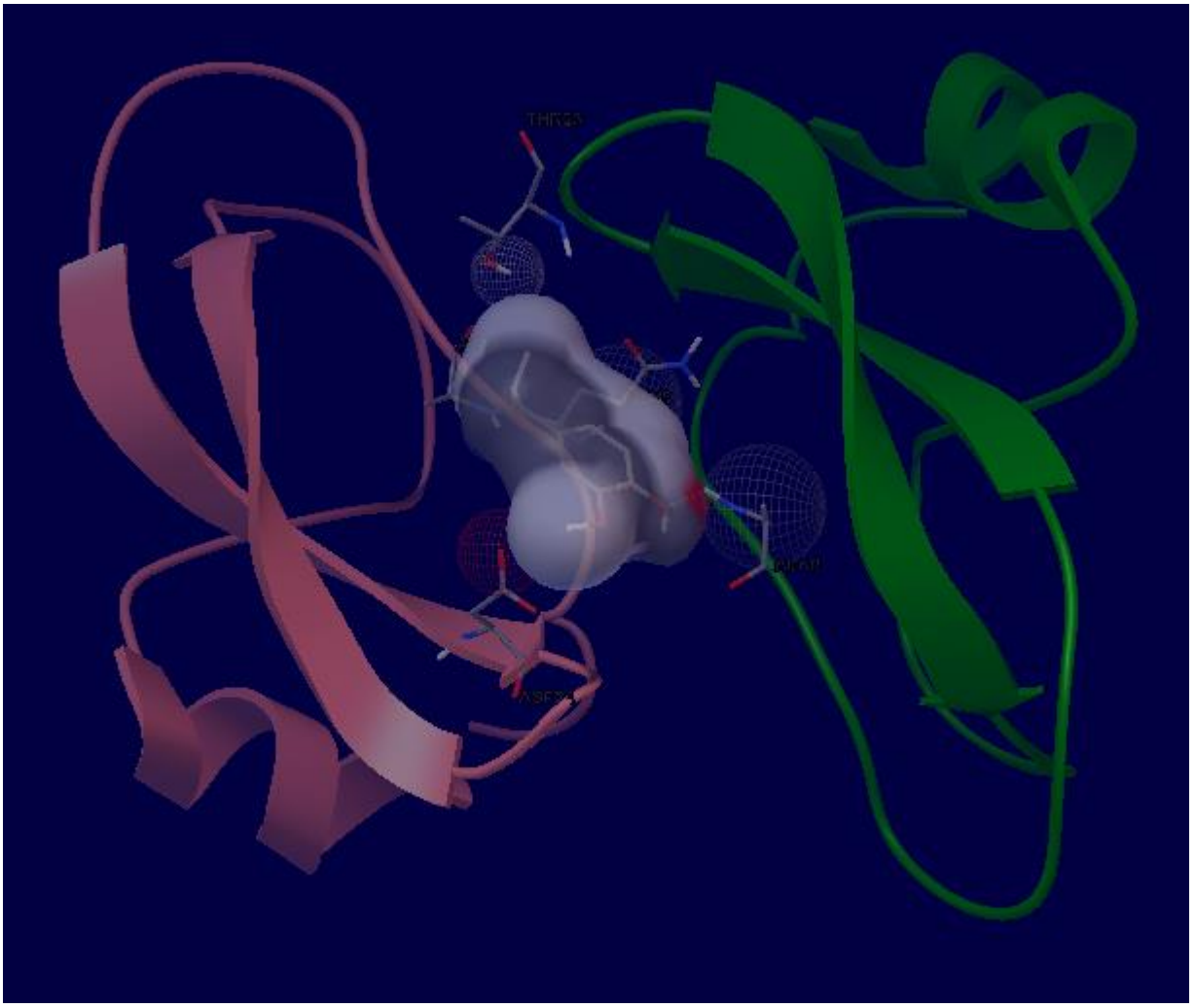

Figure 3.10 Interaction of Eugenol with APP

Figure 3.11 Illustrates the details of the binding forces of Eugenol with the surrounding amino acid residues. THR26, ALA9, GLN8 and ASP24 are the amino acid residues that bind with ligand (Eugenol) molecule.

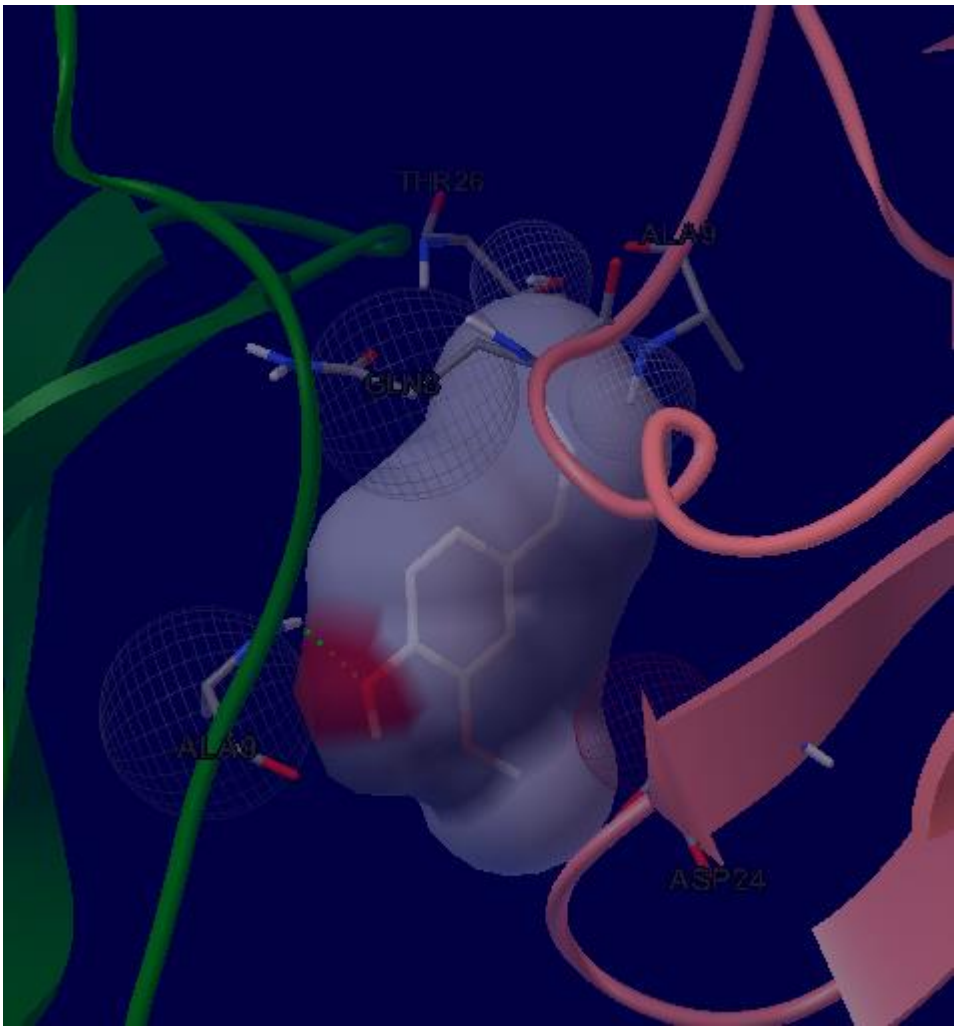

Figure 3.11 Detailed illustration of the binding forces of Eugenol with the surrounding amino acid residues of APP.

The Figure 3.12 illustrates a representative example of the clustering analysis conducted on the docked poses for Eugenol binding to APP. The root mean square deviation (RMSD) from the reference structure is found to be 42.37 Å. Here we used RMSD tolerance of 2 Å. The estimated inhibition constant (Ki) for this interaction is determined to be 3.14 mM (millimolar) at a temperature of 298.15 K.

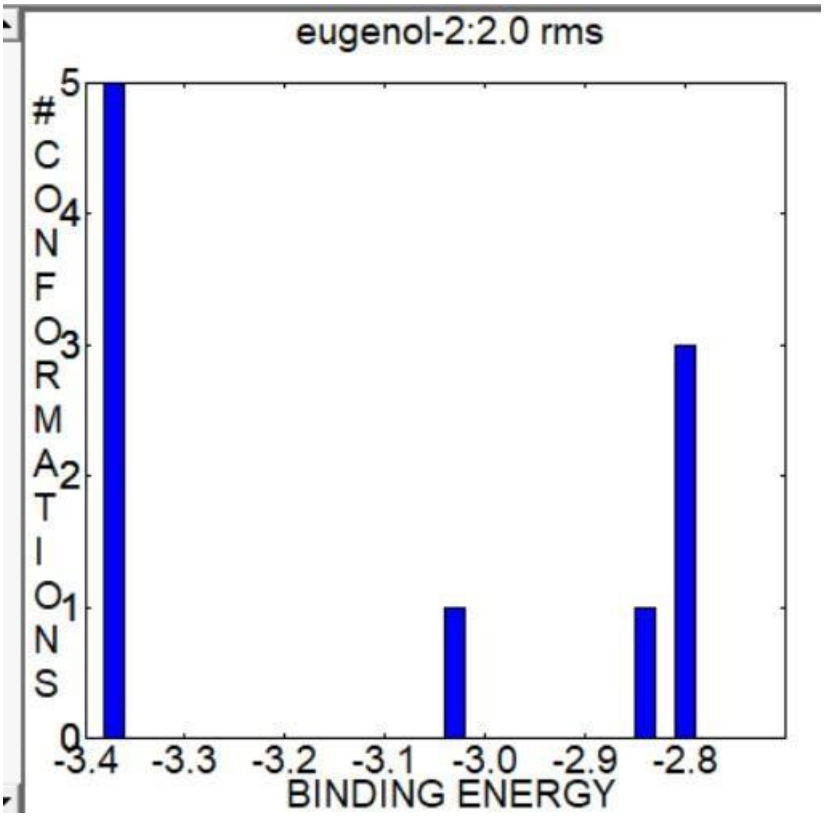

Figure 3.12 A graph representing the binding energy versus conformations in the angstrom units of Eugenol with APP.

The statistical mechanical calculations were done for the binding process of Eugenol with APP and tabulated as shown in Table 3.4. The partition function, free energy, internal energy, entropy and binding energy of the interaction were given in the table. The binding process between Eugenol and APP was spontaneous and entropy driven.

Receptor	**Ligand**	**Partition function (Q) Kcal/mol**	**Free energy (A) Kcal/mol**	**Internal energy (U) Kcal/mol**	**Entropy (S) Kcal/mol/K**	**Binding energy Kcal/mol**
APP	Eugenol	10.05	-1367.26	-3.02	4.58	-3.37

Table 3.4 The statistical mechanical analysis results of Eugenol with APP

3.1.5 ZERUMBONE WITH APP

The biomolecular recognition of Zerumbone with APP was studied by Molecular Docking using AutoDock software. According to the results, the binding process between Zerumbone and APP is primarily governed by hydrophobic interactions and hydrogen bond forces. Out of the 10 obtained docking conformations, the conformation with lowest free binding energy was selected and analyzed. The lowest binding energy is obtained for the 2nd conformations. The lowest binding energy in this Zerumbone-APP interaction is -5.58 kcal/mol. As shown in Figure 3.13 Zerumbone inserted into the APP with a free binding energy of -5.58 kcal/mol.

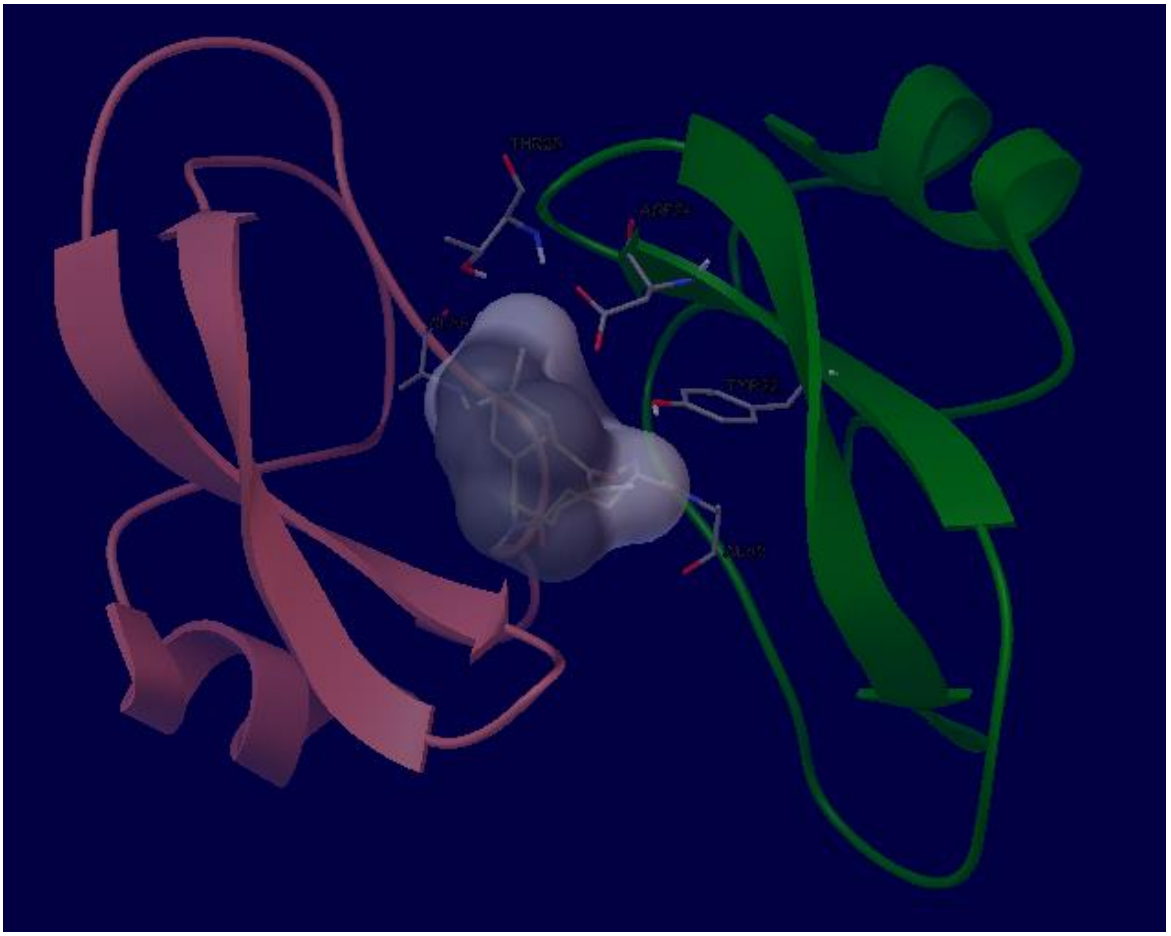

Figure 3.13 Interaction of Zerumbone with APP

Figure 3.14 Illustrates the details of the binding forces of Zerumbone with the surrounding amino acids residues. THR26, ALA9, ASP24, TYR22 and GLN8 are the various amino acid residues that bind with ligand (Zerumbone) molecule.

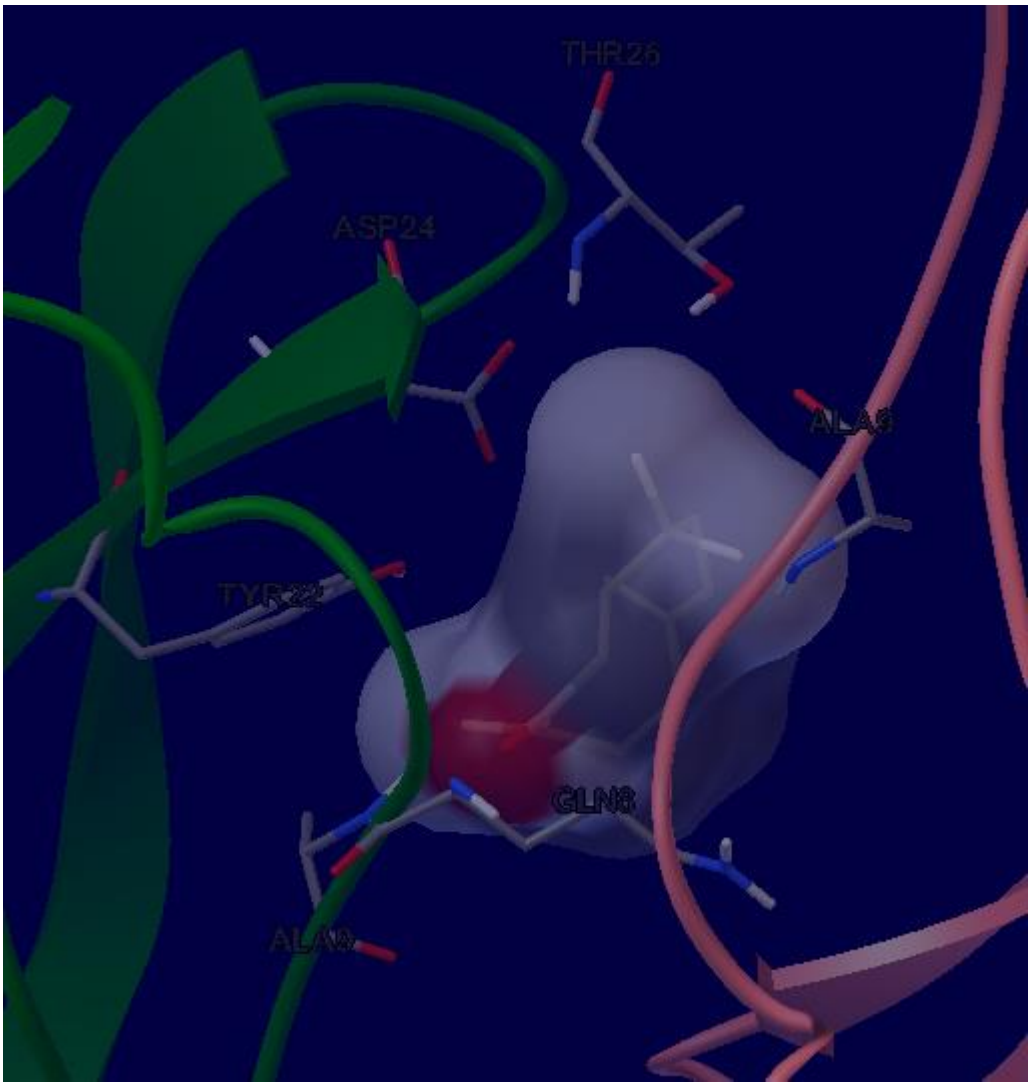

Figure 3.14 Detailed illustration of the binding forces of Zerumbone with the surrounding amino acid residues of APP.

The Figure 3.15 illustrates a representative example of the clustering analysis conducted on the docked poses for Zerumbone binding to APP. The root mean square deviation (RMSD) from the reference structure is found to be 40.97 Å. Here we used RMSD tolerance of 2 Å. The estimated inhibition constant (Ki) for this interaction is determined to be 80.67 uM (micromolar) at a temperature of 298.15 K.

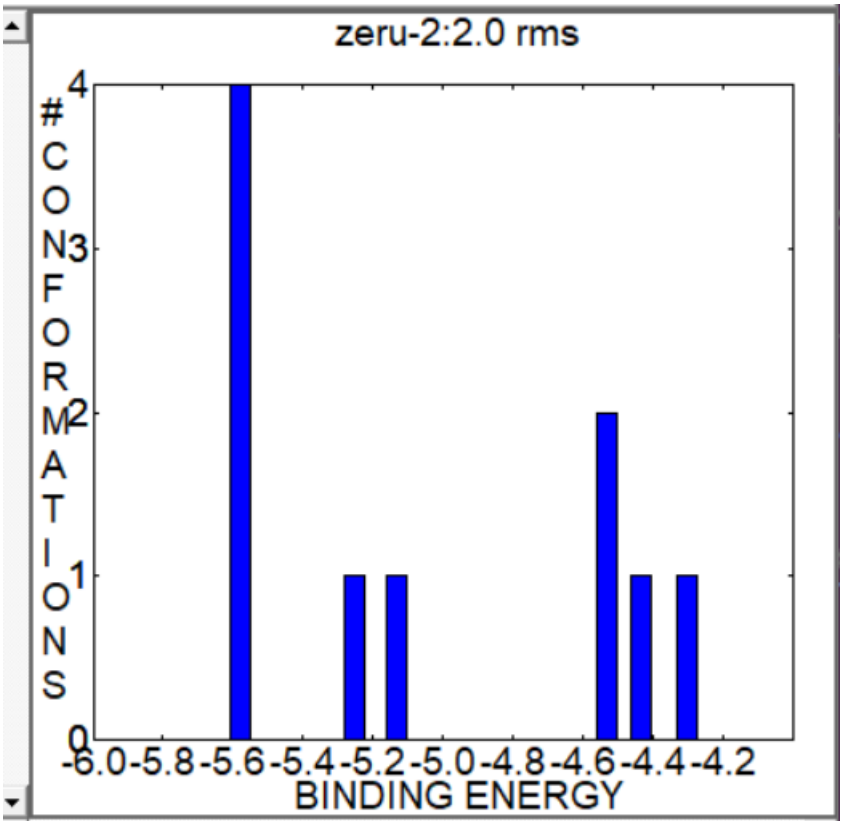

Figure 3.15 A graph representing the binding energy versus conformations in the angstrom units of Zerumbone with APP.

The statistical mechanical calculations were done for the binding process of Zerumbone with APP and tabulated as shown in Table 3.5. The partition function, free energy, internal energy, entropy and binding energy of the interaction were given in the table. The binding process between Zerumbone and APP was spontaneous and entropy driven.

Receptor	**Ligand**	**Partition function (Q) Kcal/mol**	**Free energy (A) Kcal/mol**	**Internal energy (U) Kcal/mol**	**Entropy (S) Kcal/mol/K**	**Binding energy Kcal/mol**
APP	Zerumbone	10.09	-1369.28	-5.05	4.58	-5.58

Table 3.5 The statistical mechanical analysis results of Zerumbone with APP

3.1.6 ALLICIN WITH APP

The biomolecular recognition of Allicin with APP was studied by Molecular Docking using AutoDock software. According to the results, the binding process between Allicin and APP is primarily governed by hydrophobic interactions and hydrogen bond forces. Out of the 10 obtained docking conformations, the conformation with lowest free binding energy was selected and analyzed. The lowest binding energy is obtained for the 2nd conformations. The lowest binding energy in this Allicin-APP interaction is -3.58 kcal/mol. As shown in Figure 3.16 Allicin inserted into the APP with a free binding energy of -3.58 kcal/mol.

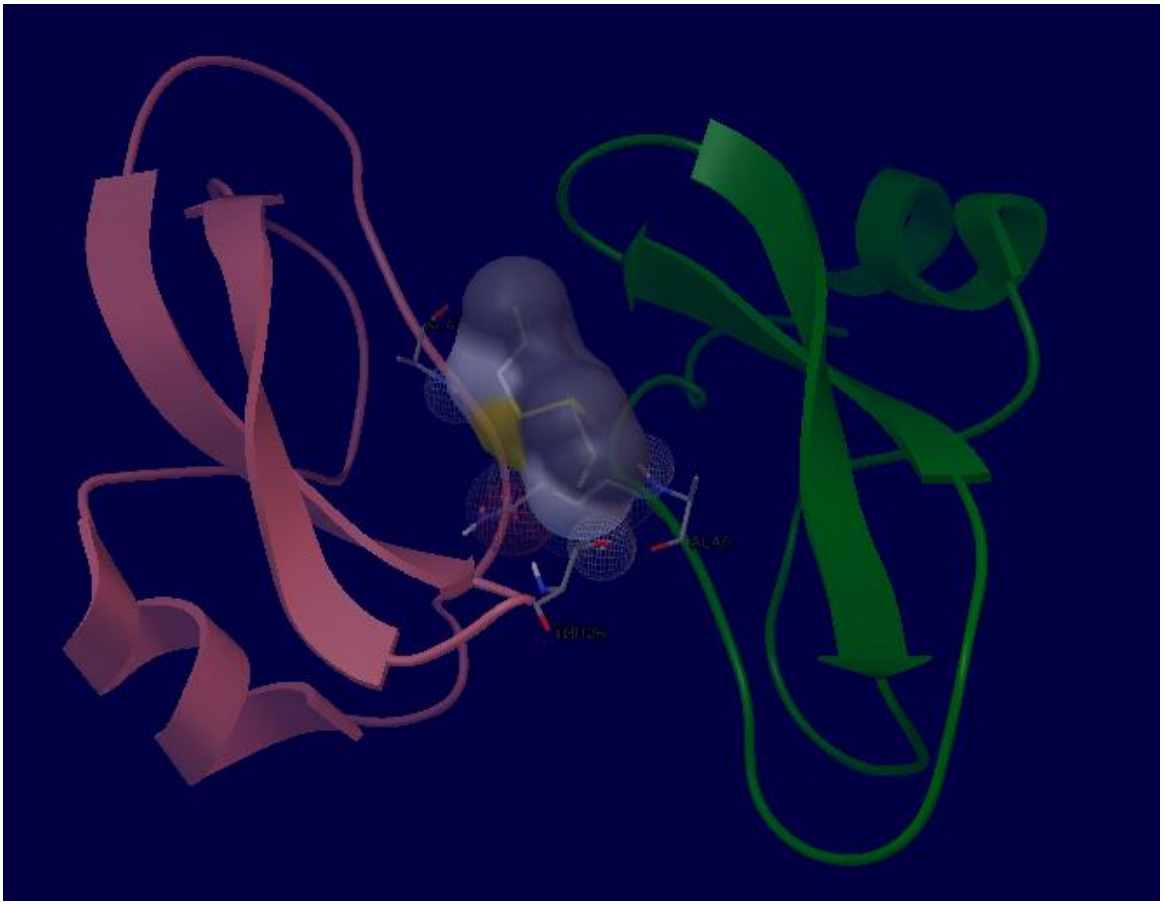

Figure 3.16 Interaction of Allicin with APP

Figure 3.17 Illustrates the details of the binding forces of Allicin with the surrounding amino acid residues. ALA9, THR26 and GLN8 are the amino acid residues that bind with ligand (Allicin) molecule.

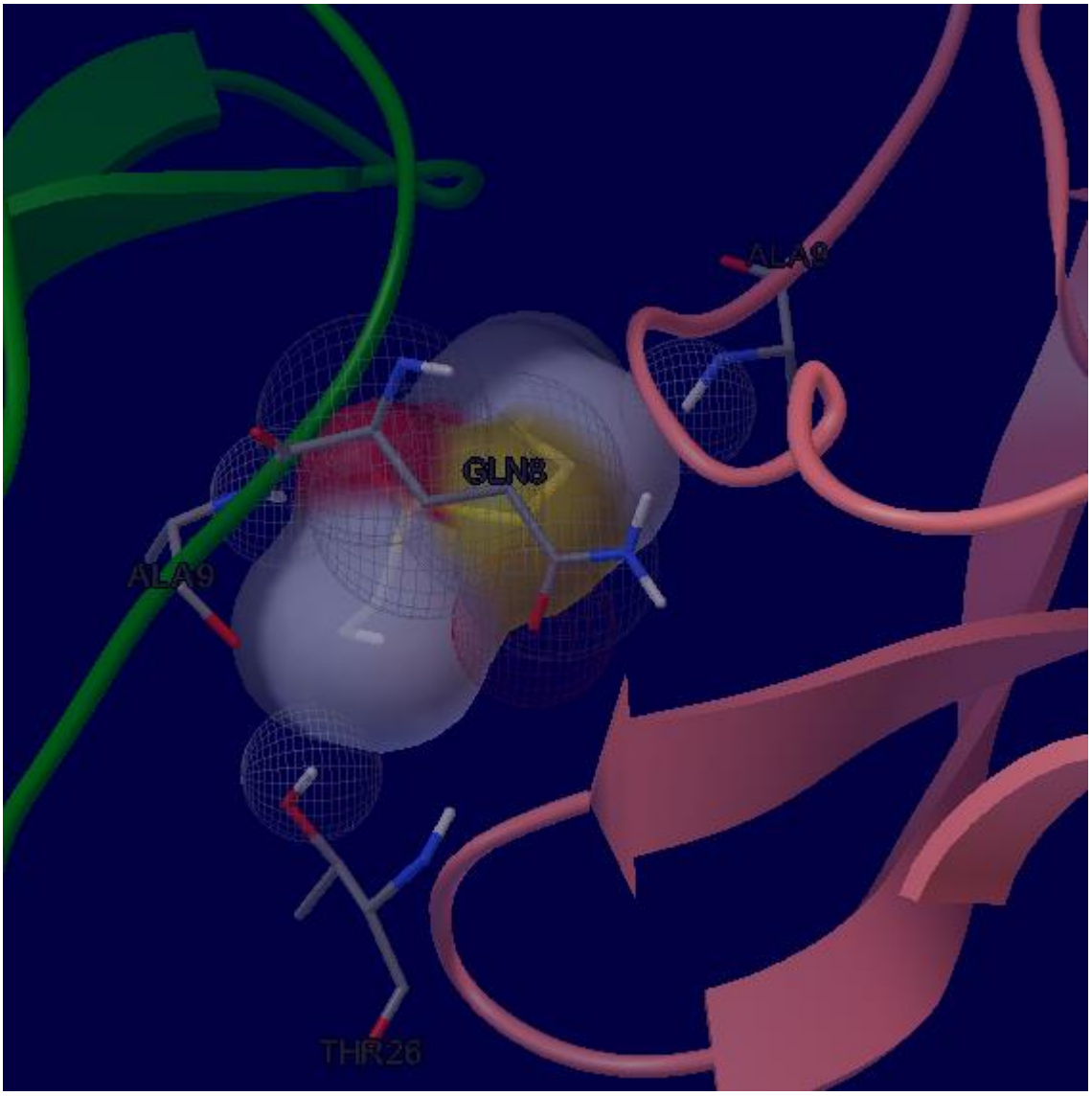

Figure 3.17 Detailed illustration of the binding forces of Allicin with the surrounding amino acid residues of APP.

The Figure 3.18 illustrates a representative example of the clustering analysis conducted on the docked poses for Allicin binding to APP. The root mean square deviation (RMSD) from the reference structure is found to be 42.79 Å. Here we used RMSD tolerance of 2 Å. The estimated inhibition constant (Ki) for this interaction is determined to be 2.37 mM (millimolar) at a temperature of 298.15 K.

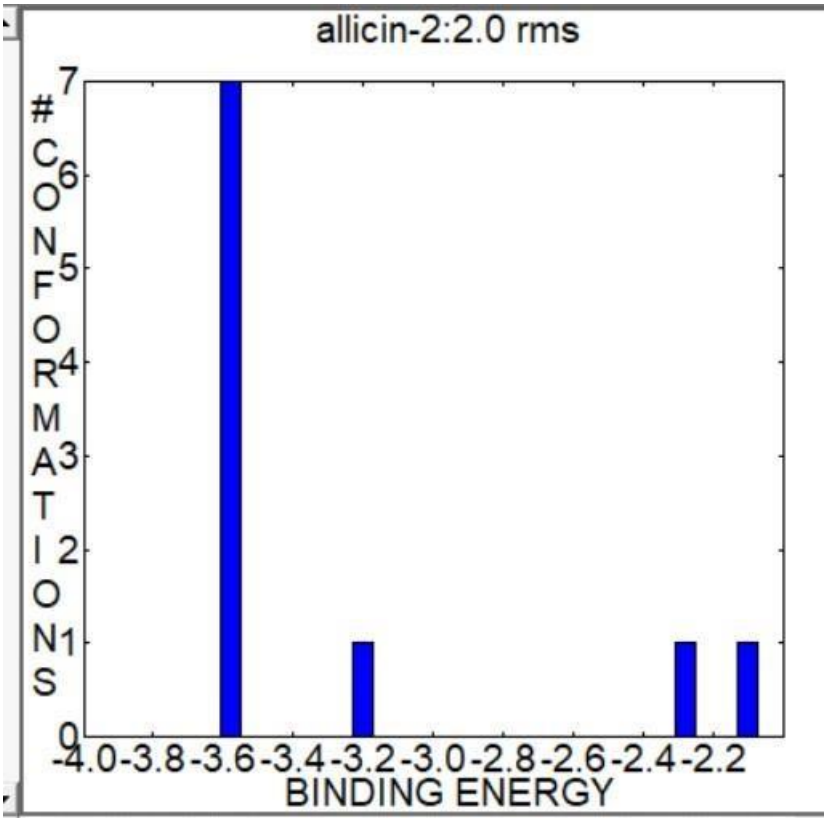

Figure 3.18 A graph representing the binding energy versus conformations in the angstrom units of Allicin with APP.

The statistical mechanical calculations were done for the binding process of Allicin with APP and tabulated as shown in Table 3.6. The partition function, free energy, internal energy, entropy and binding energy of the interaction were given in the table. The binding process between Allicin and APP was spontaneous and entropy driven.

Receptor	**Ligand**	**Partition function (Q) Kcal/mol**	**Free energy (A) Kcal/mol**	**Internal energy (U) Kcal/mol**	**Entropy (S) Kcal/mol/K**	**Binding energy Kcal/mol**
APP	Allicin	10.05	-1367.36	-3.12	4.58	-3.58

Table 3.6 The statistical mechanical analysis results of Allicin with APP

3.1.7 MYRISTICIN WITH APP

The biomolecular recognition of Myristicin with APP was studied by Molecular Docking using AutoDock software. According to the results, the binding process between Myristicin and APP is primarily governed by hydrophobic interactions and hydrogen bond forces. Out of the 10 obtained docking conformations, the conformation with lowest free binding energy was selected and analyzed. The lowest binding energy is obtained for the 8th conformations. The lowest binding energy in this Myristicin-APP interaction is -3.67 kcal/mol. As shown in Figure 3.19 Myristicin inserted into the APP with a free binding energy of -3.67 kcal/mol.

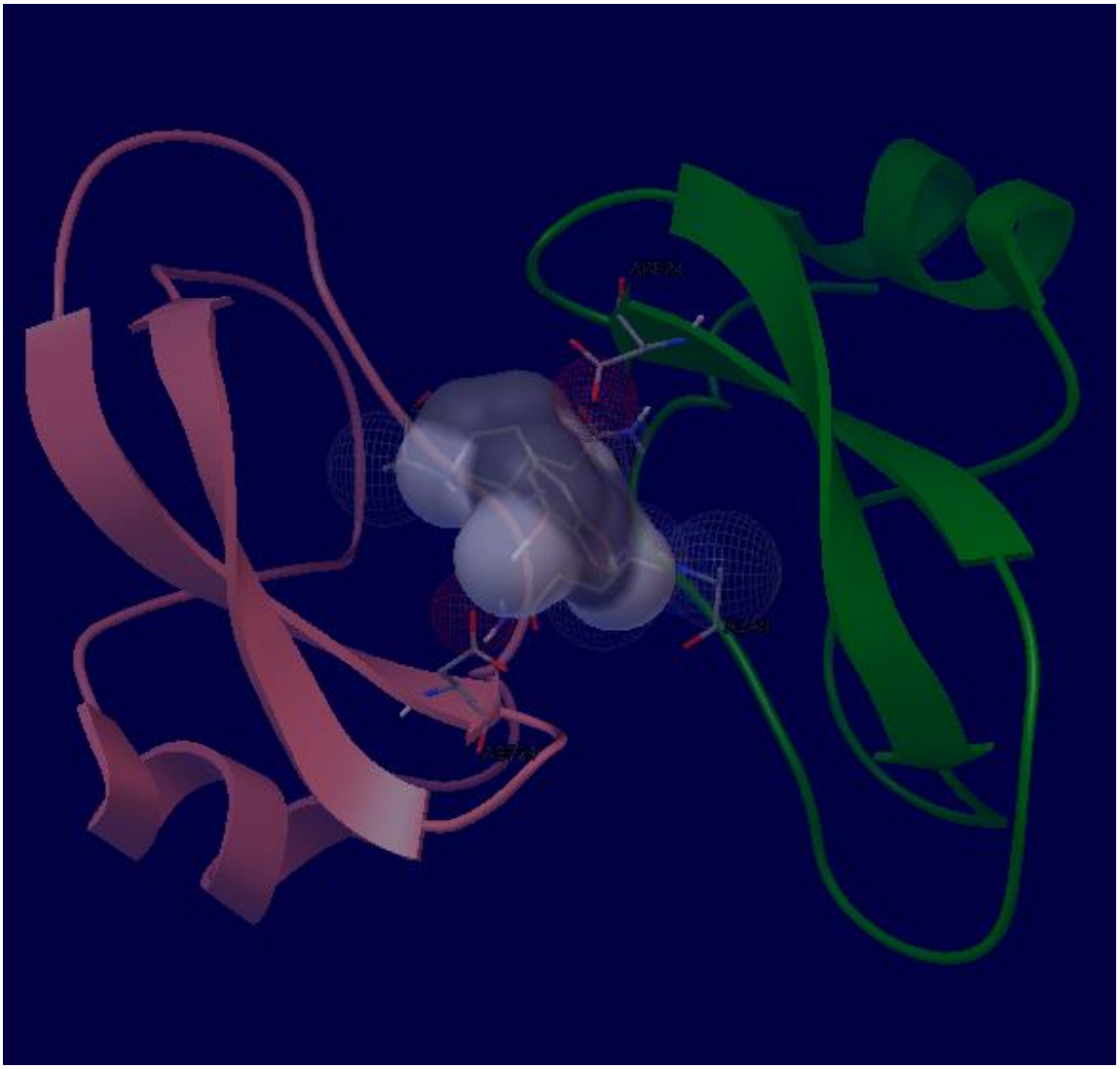

Figure 3.19 Interaction of Myristicin with APP

Figure 3.20 Illustrates the details of the binding forces of Myristicin with the surrounding amino acid residues. ASP24, ALA9 and GLN8 are the amino acid residues that bind with ligand (Myristicin) molecule.

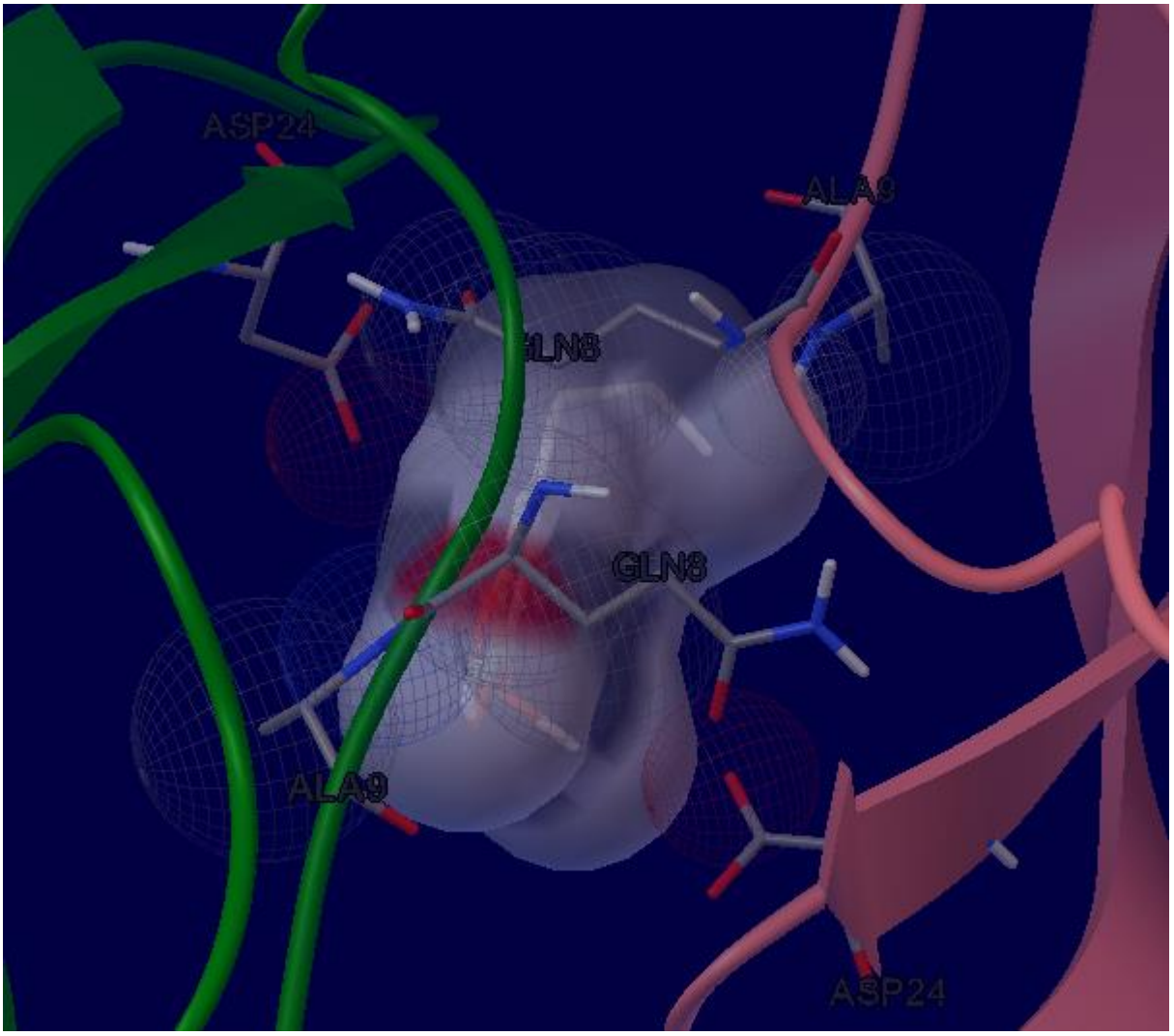

Figure 3.20 Detailed illustration of the binding forces of Myristicin with the surrounding amino acid residues of APP.

The Figure 3.21 illustrates a representative example of the clustering analysis conducted on the docked poses for Myristicin binding to APP. The root mean square deviation (RMSD) from the reference structure is found to be 42.13 Å. Here we used RMSD tolerance of 2 Å. The estimated inhibition constant (Ki) for this interaction is determined to be 2.03 mM (millimolar) at a temperature of 298.15 K.

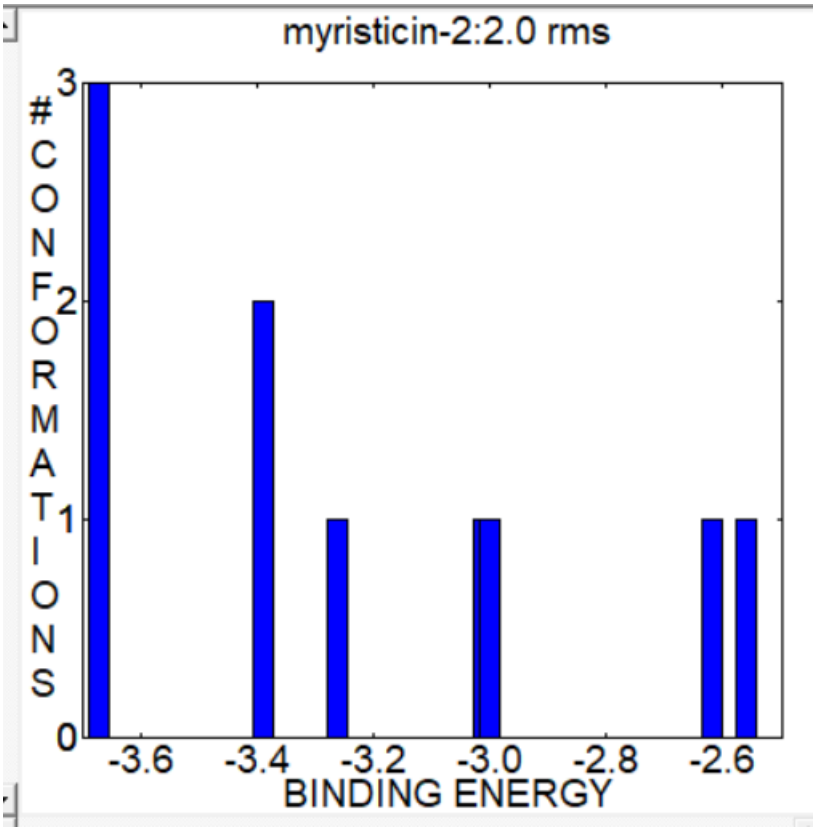

Figure 3.21 A graph representing the binding energy versus conformations in the angstrom units of Myristicin with APP.

The statistical mechanical calculations were done for the binding process of Myristicin with APP and tabulated as shown in Table 3.7. The partition function, free energy, internal energy, entropy and binding energy of the interaction were given in the table. The binding process between Myristicin and APP was spontaneous and entropy driven.

Receptor	**Ligand**	**Partition function (Q) Kcal/mol**	**Free energy (A) Kcal/mol**	**Internal energy (U) Kcal/mol**	**Entropy (S) Kcal/mol/K**	**Binding energy Kcal/mol**
APP	Myristicin	10.05	-1367.43	-3.19	4.58	-3.67

Table 3.7 The statistical mechanical analysis results of Myristicin with APP

3.1.8 CURCUMIN WITH APP

The biomolecular recognition of Curcumin with APP was studied by Molecular Docking using AutoDock software. According to the results, the binding process between Curcumin and APP is primarily governed by hydrophobic interactions and hydrogen bond forces. Out of the 10 obtained docking conformations, the conformation with lowest free binding energy was selected and analyzed. The lowest binding energy is obtained for the 2nd conformations. The lowest binding energy in this Curcumin-APP interaction is -3.84 kcal/mol. As shown in Figure 3.22 Curcumin inserted into the APP with a free binding energy of -3.84 kcal/mol.

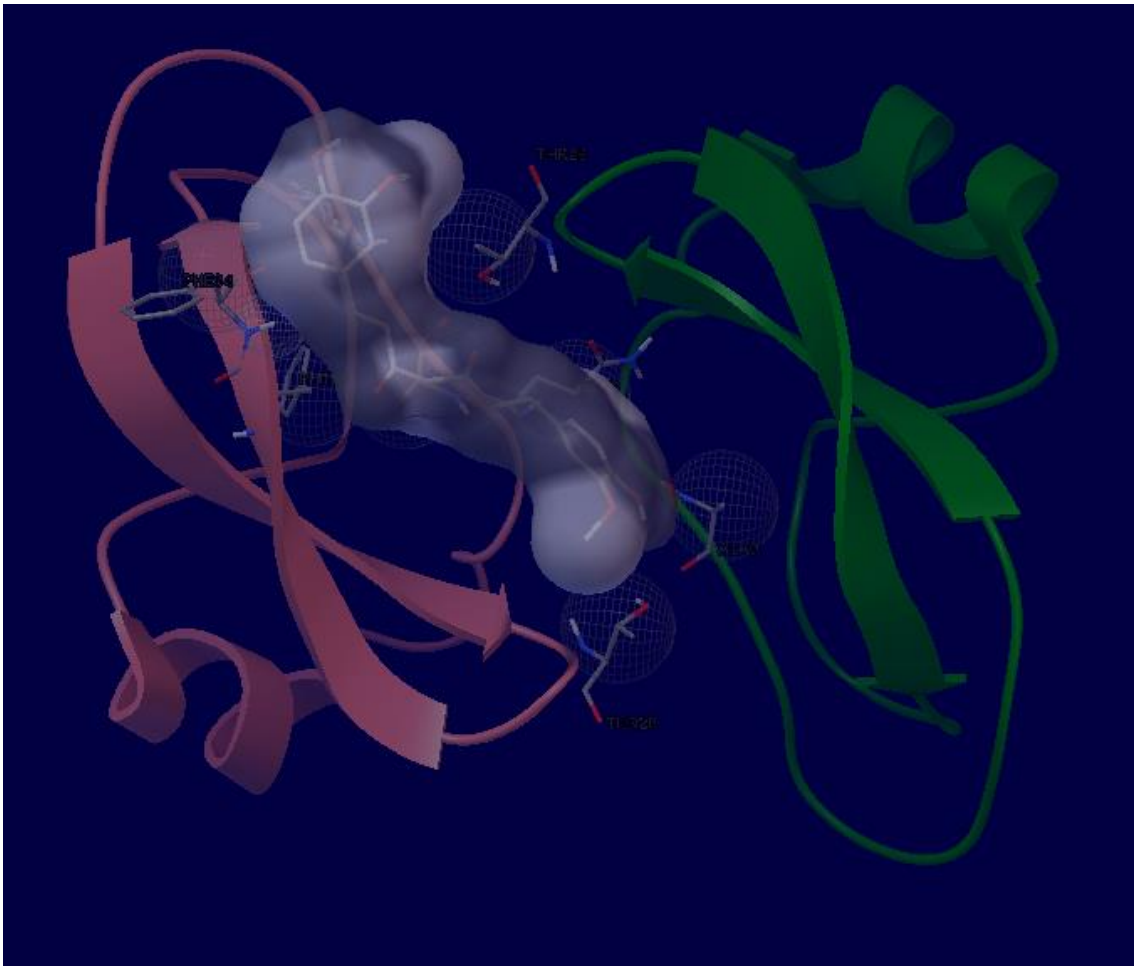

Figure 3.22 Interaction of Curcumin with APP

Figure 3.23 Illustrates the details of the binding forces of Curcumin with the surrounding amino acid residues. GLN8,ALA9, THR11, PHE33, PHE34 and THR26 are the amino acid residues that bind with ligand (Curcumin) molecule.

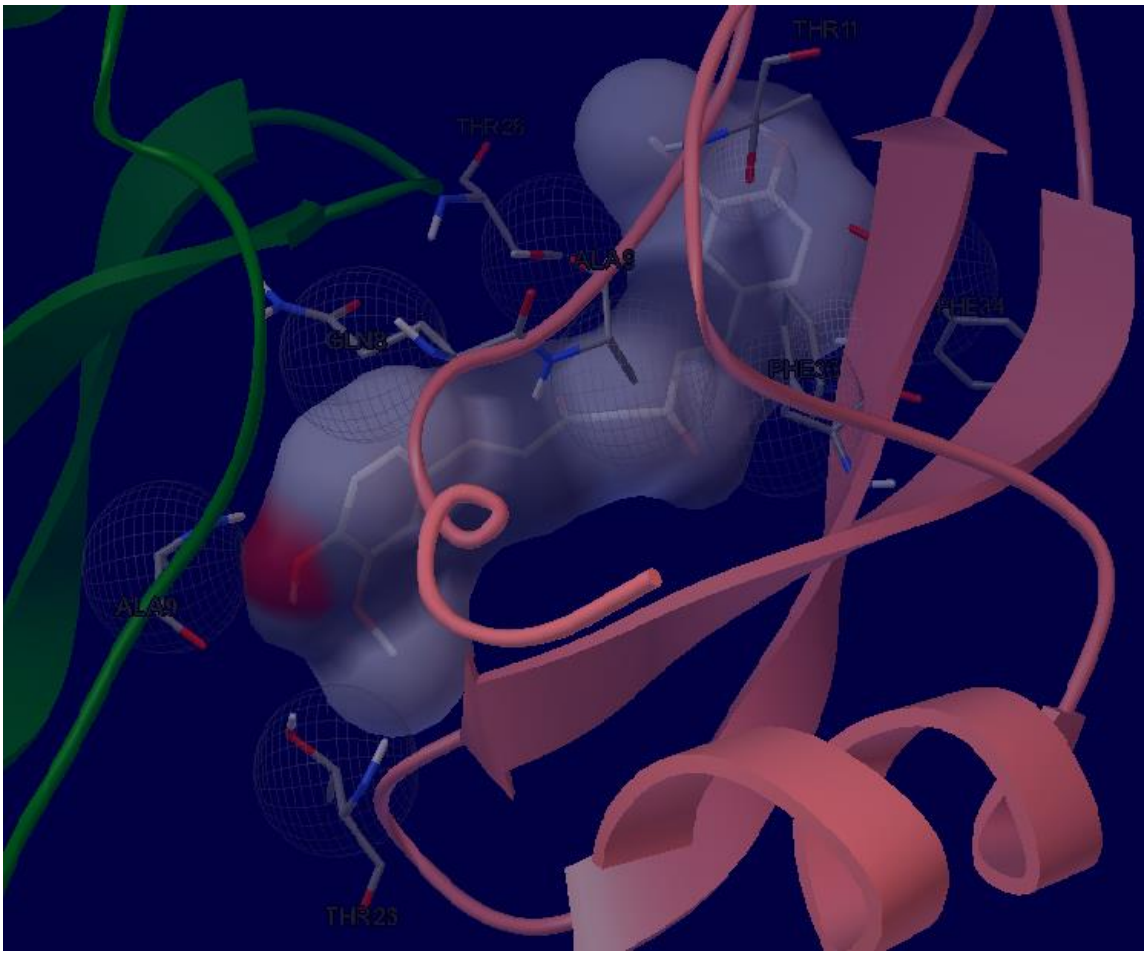

Figure 3.23 Detailed illustration of the binding forces of Curcumin with the surrounding amino acid residues of APP.

The Figure 3.24 illustrates a representative example of the clustering analysis conducted on the docked poses for Curcumin binding to APP. The root mean square deviation (RMSD) from the reference structure is found to be 39.65 Å. Here we used RMSD tolerance of 2 Å. The estimated inhibition constant (Ki) for this interaction is determined to be 1.52 mM (millimolar) at a temperature of 298.15 K.

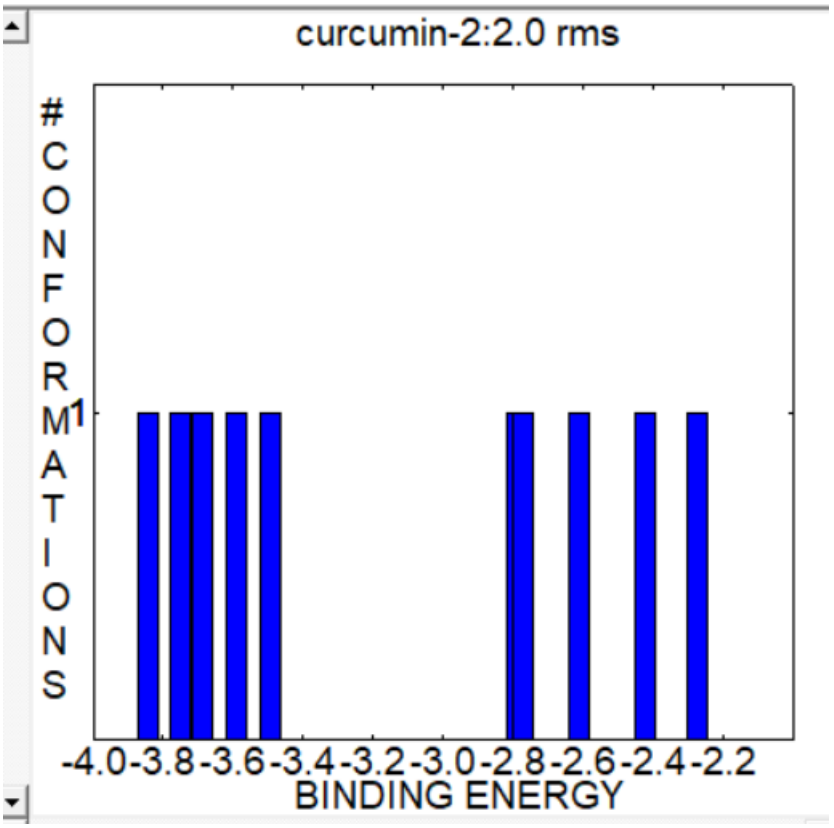

Figure 3.24 A graph representing the binding energy versus conformations in the angstrom units of Curcumin with APP.

The statistical mechanical calculations were done for the binding process of Curcumin with APP and tabulated as shown in Table 3.8. The partition function, free energy, internal energy, entropy and binding energy of the interaction were given in the table. The binding process between Curcumin and APP was spontaneous and entropy driven.

Receptor	**Ligand**	**Partition function (Q) Kcal/mol**	**Free energy (A) Kcal/mol**	**Internal energy (U) Kcal/mol**	**Entropy (S) Kcal/mol/K**	**Binding energy Kcal/mol**
APP	Curcumin	10.05	-1367.36	-3.12	4.58	-3.84

Table 3.8 The statistical mechanical analysis results of Curcumin with APP

3.2 STATISTICAL MECHANICAL ANALYSIS

The overall result of statistical mechanical analysis of the eight studied ligand molecules with APP are given in Table 3.9. From the table it is clear that the negative binding free energy is maximum for Piperine (-5.77 Kcal/mol) and least for Eugenol (-3.37 Kcal/mol) at 298.15 K.

RECEPTOR	LIGAND	PARTITION FUNCTION (Q) Kcal/mol	FREE ENERGY (A) Kcal/mol	INTERNAL ENERGY (U) Kcal/mol	ENTROPY (S) Kcal/mol/K	BINDING ENERGY Kcal/mol
APP	Piperine	10.09	-1369.67	-5.43	4.58	-5.77
	Cineole	10.07	-1368.43	-4.19	4.58	-4.47
	Cinnamald-ehyde	10.07	-1368.17	-3.93	4.58	-3.96
	Eugenol	10.05	-1367.26	-3.02	4.58	-3.37
	Zerumbon-E	10.09	-1369.28	-5.05	4.58	-5.58
	Allicin	10.05	-1367.36	-3.12	4.58	-3.58
	Myristicin	10.05	-1367.43	-3.19	4.58	-3.67
	Curcumin	10.05	-1367.36	-3.12	4.58	-3.84

Table 3.9 Overall result of statistical mechanical analysis of the eight studied ligand molecules with APP

CHAPTER 4

CONCLUSION

Based on the results of the molecular modeling and docking study, the binding interactions between Amyloid-beta precursor protein (APP) and various bioactive compounds found in spices were investigated. The binding energies of these molecules with APP were calculated, and the complexes with favorable negative binding energies were identified. The overall results, as shown in Table 3.9, indicate that the binding free energy is highest for Piperine (-5.77 kcal/mol) and lowest for Eugenol (-3.37 kcal/mol) at 298.15 K. These findings suggest that Piperine has the strongest binding affinity towards APP among the studied ligand molecules. Cineole, Cinnamaldehyde, Zerumbone, Allicin, Myristicin, and Curcumin also exhibit relatively favorable binding energies, indicating potential interactions with APP. However, Eugenol shows a comparatively weaker binding affinity. The results of this study provide valuable insights into the potential bioactive compounds present in spices that can interact with and bind to APP. Since APP plays a crucial role in the pathogenesis of Alzheimer's disease, the identified compounds hold promise for the development of novel therapeutic interventions targeting this neurodegenerative disorder. Further exploration and investigation of these identified compounds, particularly Piperine, could lead to the design and development of drugs that can modulate APP function and potentially mitigate the progression of Alzheimer's disease. However, it is important to note that these findings are based on computational modeling and docking techniques, and experimental validation is necessary to confirm the binding interactions and therapeutic potential of these compounds.

REFERENCE

[1] Prof Clive Ballard, MRCPsych; Serge Gauthier, MD; Anne Corbert, PhD; Carol Baryan, MD; Dag Aarsland, MD; Emma Jones, PhD. Alzheimer's disease. Published: March 02, 2011 DOI: https://doi.org/10.1016/S0140-6736(10)61349-9

[2] Alzheimer's disease fact sheet. National Institute on Aging. https://www.nia.nih.gov/health/alzheimers-disease-fact-sheet.

[3] Alzheimer's Association - What isAlzheimer's Disease? Symptoms & Causes | alz.org

[4] Jankovic J, et al., eds. Alzheimer disease and other dementias. In: Bradley and Daroff's Neurology in Clinical Practice. 8th ed. Elsevier; 2022.

[5] Rogers, Kara. Biomolecule. Encyclopedia Britannica, https://www.britannica.com/science/biomolecule. Accessed 5 June 2021.

[6] Damodaran, Srinivasan, and Kirk L. Parkin. Amino acids, peptides, and proteins. Fennema's food chemistry. CRC Press, 2017. Pages 235-356.

[7] Francisco J. Barba, María J. Esteve, Ana Frígola, Chapter 11 - Bioactive Components from Leaf Vegetable Products, Editor(s): Atta-ur-Rahman,Studies in Natural Products Chemistry, Elsevier, Volume 41, 2014, Pages 321-346.

[8] Alexander Yashin, Yakov Yashin, Xiaoyan Xia and Boris Nemzer Antioxidant Activity of Spices and Their Impact on Human Health: A Review"Published: 15 September2017

[9] Richard J. O'Brien and Philip C. Wong Amyloid Precursor Protein Processing and Alzheimer's Disease.

[10] Tharp WG, Sarkar IN (April 2013). Origins of amyloid-β. BMC Genomics. 14 (1): 290. doi:10.1186/1471-2164-14-290. PMC 3660159. PMID 23627794.

[11] Baumkotter F., Schmidt N., Vargas C., Schilling S., Weber R., Wagner K., Fiedler S., Klug W., Radzimanowski J., Nickolaus S., Keller S., Eggert S., Wild K., Kins S. Amyloid precursor protein dimerization and synaptogenic function depend on copper binding to the growth factor-like domain.

[12] Yoshikai S, Sasaki H, Doh-ura K, Furuya H, Sakaki Y (Mar 1990). Genomic organization of the human amyloid beta-protein precursor gene. Gene. 87 (2): 257–63. doi:10.1016/0378-1119(90)90310-N. PMID 2110105.

[13] Lamb BT, Sisodia SS, Lawler AM, Slunt HH, Kitt CA, Kearns WG, Pearson PL, Price DL, Gearhart JD (Sep 1993). Introduction and expression of the 400 kilobase amyloid precursor protein gene in transgenic mice [corrected]. Nature Genetics. 5 (1): 22–30. doi:10.1038/ng0993-22. PMID 8220418. S2CID 42752531.

[14] Matsui T, Ingelsson M, Fukumoto H, Ramasamy K, Kowa H, Frosch MP, Irizarry MC, Hyman BT (Aug 2007). Expression of APP pathway mRNAs and proteins in Alzheimer's disease. Brain Research. 1161: 116–23. doi:10.1016/j.brainres.2007.05.050. PMID 17586478. S2CID 26901380.

[15] Goate A, Chartier-Harlin MC, Mullan M, Brown J, Crawford F, Fidani L, Giuffra L, Haynes A, Irving N, James L (Feb 1991). Segregation of a missense mutation in the amyloid precursor protein gene with familial Alzheimer's disease. Nature. 349 (6311): 704–6. Bibcode:1991Natur.349..704G. doi:10.1038/349704a0. PMID 1671712. S2CID 4336069.

[16] Murrell J, Farlow M, Ghetti B, Benson MD (Oct 1991). "A mutation in the amyloid precursor protein associated with hereditary Alzheimer's disease". Science. 254 (5028): 97–9. Bibcode:1991Sci...254...97M. doi:10.1126/science.1925564. PMID 1925564.

[17] Chartier-Harlin MC, Crawford F, Houlden H, Warren A, Hughes D, Fidani L, Goate A, Rossor M, Roques P, Hardy J (Oct 1991). Early-onset Alzheimer's disease caused by mutations at codon 717 of the beta-amyloid precursor protein gene. Nature. 353 (6347): 844–6. Bibcode:1991Natur.353..844C. doi:10.1038/353844a0. PMID 1944558. S2CID 4345311.

[18] Lloyd, GM; Trejo-Lopez, JA; Xia, Y; McFarland, KN; Lincoln, SJ; Ertekin-Taner, N; Giasson, BI; Yachnis, AT; Prokop, S (12 March 2020). Prominent amyloid plaque pathology and cerebral amyloid angiopathy in APP V717I (London) carrier - phenotypic variability in autosomal dominant Alzheimer's disease. Acta Neuropathologica Communications. 8 (1): 31. doi:10.1186/s40478-020-0891-3. PMC 7068954. PMID 32164763.

[19] Hynes, T. R., Randal, M., Kennedy, L., Eigenbrot, C., & Kossiakoff, A. A. (1990). X-ray crystal structure of the protease inhibitor domain of Alzheimer's amyloid.beta.-protein precursor. Biochemistry, 29(43), 10018–10022. https://doi.org/10.1021/bi00495a002

[20] Derosa, G., Maffioli, P., Sahebkar, A. (2016). Piperine and Its Role in Chronic Diseases. In: Gupta, S., Prasad, S., Aggarwal, B. (eds) Anti-inflammatory Nutraceuticals and Chronic Diseases. Advances in Experimental Medicine and Biology, vol 928. Springer, Cham. https://doi.org/10.1007/978-3-319-41334-1_8.

[21] Epstein, William W.; Netz, David F.; Seidel, Jimmy L. (1993). Isolation of Piperine from Black Pepper. J. Chem. Educ. 70 (7): 598. Bibcode:1993JChEd..70..598E. doi:10.1021/ed070p598.

[22] McNamara, F. N.; Randall, A.; Gunthorpe, M. J. (March 2005). Effects of piperine, the pungent component of black pepper, at the human vanilloid receptor (TRPV1). British Journal of Pharmacology. 144 (6): 781–790. doi:10.1038/sj.bjp.0706040. PMC 1576058. PMID 15685214.

[23] Selvendiran K, Sakthisekaran D (2004) Chemopreventive effect of piperine on modulating lipid peroxidation and membrane bound enzymes in benzo(a)pyrene induced lung carcinogenesis. Biomed Pharmacother 58:264–267.

[24] Vaibhav K, Shrivastava P, Javed H, Khan A, Ahmed ME, Tabassum R, Khan MM, Khuwaja G, Islam F, Siddiqui MS, Safhi MM, Islam F (2012) Piperine suppresses cerebral ischemia-reperfusion induced inflammation through the repression of COX-2, NOS-2, and NF-κB in middle cerebral artery occlusion rat model. Mol Cell Biochem 367(1–2):73–84.

[25] Srinivasan K (2007) Black pepper and its pungent principle-piperine: a review of diverse physiological effects. Crit Rev Food Sci Nutr 47(8):735–748.

[26] Structure of Piperine: https://pubchem.ncbi.nlm.nih.gov/compound/Piperine

[27] George A. Burdock: Fenaroli's Handbook of Flavor Ingredients, Sixth Edition. CRC Press, 2009, ISBN 978-1-4200-9086-4, p.292

[28] John ApSimon: The Total Synthesis of Natural Products. John Wiley & Sons, 2009, ISBN 978-0-470-12951-7, p.134

[29] Günther Ohloff: Fragrances and the Sense of Smell The Molecular World of Fragrances. Springer-Verlag, 2013, ISBN 978-3-662-09768-7, p.223

[30] Structure of 1,4-Cineole: https://pubchem.ncbi.nlm.nih.gov/compound/1_4-Cineole

[31] Rao, P. S., & Gan, S. H. (2014). Cinnamon: A Multifaceted Medicinal Plant. Evidence-based Complementary and Alternative Medicine, 2014, 1–12. https://doi.org/10.1155/2014/642942

[32] "Cinnamon". Transport Information Service. Gesamtverband der Deutschen Versicherungswirtschaft e.V. Retrieved 2007-10-23.

[33] Gutzeit, Herwig (2014). Plant Natural Products: Synthesis, Biological Functions and Practical Applications. Wiley. pp. 19–21. ISBN 978-3-527-33230-4.

[34] Inuzuka, K. (1961). π Electronic Structure of Cinnamaldehyde. *Bulletin of the Chemical Society of Japan*, *34*(11), 1557–1560. https://doi.org/10.1246/bcsj.34.1557

[35] Fahlbusch, Karl-Georg; Hammerschmidt, Franz-Josef; Panten, Johannes; Pickenhagen, Wilhelm; Schatkowski, Dietmar; Bauer, Kurt; Garbe, Dorothea; Surburg, Horst (2003). "Flavors and Fragrances". Ullmann's Encyclopedia of Industrial Chemistry. doi:10.1002/14356007.a11_141. ISBN 978-3-527-30673-2.

[36] Cabello, Gema; Funkhouser, Gary P.; Cassidy, Juanita; Kiser, Chad E.; Lane, Jim; Cuesta, Angel (2013-05-01). "CO and trans-cinnamaldehyde as corrosion inhibitors of I825, L80-13Cr and N80 alloys in concentrated HCl solutions at high pressure and temperature". Electrochimica Acta. 97: 1–9. doi:10.1016/j.electacta.2013.03.011. hdl:2164/2891. ISSN 0013-4686.

[37] Structure of Cinnamaldehyde: https://pubchem.ncbi.nlm.nih.gov/compound/637511

[38] "Eugenol". PubChem, US National Library of Medicine. 16 October 2021. Retrieved 24 October 2021.

[39] "Constituents of the essential oil from leaves and buds of clove (Syzigium caryophyllatum L.) Alston" (PDF). Bangladesh Council of Scientific and Industrial Research BCSIR Laboratories. 4: 451–454.

[40] Mallavarapu GR, Ramesh S, Chandrasekhara RS, Rajeswara Rao BR, Kaul PN, Bhattacharya AK (1995). "Investigation of the essential oil of cinnamon leaf grown at Bangalore and Hyderabad". Flavour and Fragrance Journal. 10 (4): 239–242. doi:10.1002/ffj.2730100403.

[41] Yield and Oil Composition of 38 Basil (Ocimum basilicum L.) Accessions Grown in Mississippi Archived 15 October 2010 at the Wayback Machine

[42] "Typical G.C. for bay leaf oil". Thegoodscentscompany.com. Archived from the original on 17 March 2014. Retrieved 27 April 2014.

[43] Wishart, David S.; Guo, An Chi; Oler, Eponine; Wang, Fel; Anjum, Afia; Peters, Harrison; Dizon, Raynard; Sayeeda, Zinat; Tian, Siyang; Lee, Brian L.; Berjanskii, Mark; Mah, Robert; Yamamoto, Mai; Jovel Castillo, Juan; Torres Calzada, Claudia; Hiebert Giesbrecht, Mickel; Lui, Vicki W.; Varshavi, Dorna; Varshavi, Dorsa; Allen, Dana; Arndt, David; Khetarpal, Nitya; Sivakumaran, Aadhavya; Harford, Karxena; Sanford, Selena; Yee, Kristen; Cao, Xuan; Budinsky, Zachary; Liigand, Jaanus; Zhang, Lun; Zheng, Jiamin; Mandal, Rupasri; Karu, Naama; Dambrova, Maija; Schiöth, Helgi B.; Gautam, Vasuk. "Showing metabocard for Eugenol (HMDB0005809)". Human Metabolome Database, HMDB. 5.0.

[44] Sell AB, Carlini EA (1976). "Anesthetic action of methyleugenol and other eugenol derivatives". Pharmacology. 14 (4): 367–77. doi:10.1159/000136617. PMID 935250.

[45] Jadhav BK, Khandelwal KR, Ketkar AR, Pisal SS (February 2004). "Formulation and evaluation of mucoadhesive tablets containing eugenol for the treatment of periodontal diseases". Drug Development and Industrial Pharmacy. 30 (2): 195–203. doi:10.1081/DDC-120028715. PMID 15089054. S2CID 19138725

[46] "Eugenol (clove oil)". LiverTox, US National Institute of Diabetes and Digestive and Kidney Diseases. 28 October 2018. PMID 31869191. Retrieved 24 October 2021.

[47] Structure of Eugenol: https://pubchem.ncbi.nlm.nih.gov/compound/3314

[48] Kitayama, T. (2011). Attractive Reactivity of a Natural Product, Zerumbone. Bioscience, Biotechnology, and Biochemistry, 75(2), 199–207. https://doi.org/10.1271/bbb.100532

[49] Padalia R.C., Verma R.S., Chauhan A., Singh V.R., Goswami P., Singh S., Verma S.K., Luqman S., Chanotiya C.S., Darokar M.P. Zingiber zerumbet (L.) Roscoe ex Sm. from northern India: Potential source of zerumbone rich essential oil for antiproliferative and antibacterial applications. Ind. Crops Prod. 2018;112:749–754. doi: 10.1016/j.indcrop.2018.01.006.

[50] Moreira Da Silva T., Pinheiro C.D., Puccinelli Orlandi P., Pinheiro C.C., Soares Pontes G. Zerumbone from Zingiber zerumbet (L.) smith: A potential prophylactic and therapeutic agent against the cariogenic bacterium Streptococcus mutans. BMC Complement. Altern. Med. 2018;18:301. doi: 10.1186/s12906-018-2360-0.

[51] Girisa S., Shabnam B., Monisha J., Fan L., Halim C.E., Arfuso F., Ahn K.S., Sethi G., Kunnumakkara A.B. Potential of zerumbone as an anti-cancer agent. Molecules. 2019;24:734. doi: 10.3390/molecules24040734.

[52] Veena K.S., Gopalan G., Madhukrishnan M., Varughese S., Radhakrishnan K.V., Lankalapalli R.S. Putative biomimetic route to 8-oxabicyclo[3.2.1]octane motif from a humulene sesquiterpenoid zerumbone. Org. Lett. 2020;22:6409–6413. doi: 10.1021/acs.orglett.0c02220.

[53] Deng M., Yun X., Ren S., Qing Z., Luo F. Plants of the genus Zingiber: A review of their ethnomedicine, phytochemistry and pharmacology. Molecules. 2022;27:2826. doi: 10.3390/molecules27092826.

[54] Tian M., Wu X., Hong Y., Wang H., Deng G., Zhou Y. Comparison of chemical composition and bioactivities of essential oils from fresh and dry rhizomes of Zingiber zerumbet (L.) Smith. Biomed Res. Int. 2020;2020:9. doi: 10.1155/2020/9641284.

[55] Albaayit S.F.A., Maharjan R., Abdullah R., Noor M.H.M. Evaluation of anti-methicillin-resistant Staphylococcus aureus property of zerumbone. J. Appl. Biomed. 2022;20:15–21. doi: 10.32725/jab.2022.002.

[56] Woo H.J., Yang J.Y., Lee P., Kim J.B., Kim S.H. Zerumbone inhibits Helicobacter pylori urease activity. Molecules. 2021;26:2663. doi: 10.3390/molecules26092663.

[57] Sharifi-Rad M., Varoni E.M., Salehi B., Sharifi-Rad J., Matthews K.R., Ayatollahi S.A., Kobarfard F., Ibrahim S.A., Mnayer D., Zakaria Z.A., et al. Plants of the genus Zingiber as a source of bioactive phytochemicals: From tradition to pharmacy. Molecules. 2017;22:2145. doi: 10.3390/molecules22122145.

[58] Akhtar N.M.Y., Jantan I., Arshad L., Haque M.A. Standardized ethanol extract, essential oil and zerumbone of Zingiber zerumbet rhizome suppress phagocytic activity of human neutrophils. BMC Complement. Altern. Med. 2019;19:331. doi:10.1186/s12906-019-2748-5.

[59] Rana V.S., Verdeguer M., Blazquez M.A. Chemical composition of the essential oil of Zingiber zerumbet var darcyi. Nat. Prod. Commun. 2012;7:1369–1370. doi: 10.1177/1934578X1200701031.

[60] Wu Y., Guo S.S., Huang D.Y., Wang C.F., Wei J.Y., Li Z.H., Sun J.S., Bai J.F., Tian Z.F., Wang P.J., et al. Contact and repellant activities of zerumbone and its analogues from the essential oil of Zingiber zerumbet (L.) smith against Lasioderma serricorne. J. Oleo Sci. 2017;66:399–405. doi: 10.5650/jos.ess16166.

[61] Structure of Zerumbone: https://pubchem.ncbi.nlm.nih.gov/compound/Zerumbone

[62] Block, E. (1985). The Chemistry of Garlic and Onions. Scientific American, 252(3), 114–118. https://doi.org/10.1038/scientificamerican0385-114

[63] Kourounakis, P. N., & Rekka, E. A. (1991). Effect on active oxygen species of alliin and Allium sativum (garlic) powder. PubMed, 74(2), 249–252. https://pubmed.ncbi.nlm.nih.gov/1667340

[64] Nikolic V, Stankovic M, Nikolic L, Cvetkovic D (January 2004). "Mechanism and kinetics of synthesis of allicin". Die Pharmazie. 59 (1): 10–4. PMID 14964414.

[65] Ilic, D., Nikolić, V., Nikolić, L., Stanković, M., Stanojević, L. P., & Cakić, M. D. (2011). Allicin and related compounds: Biosynthesis, synthesis and pharmacological activity. Facta Universitatis, 9(1), 9–20. https://doi.org/10.2298/fupct1101009i

[66] Borlinghaus, J., Albrecht, F., Gruhlke, M. C., Nwachukwu, I. D., & Slusarenko, A. J. (2014). Allicin: Chemistry and Biological Properties. Molecules, 19(8), 12591–12618. https://doi.org/10.3390/molecules190812591

[67] Rabinkov, A., Miron, T., Konstantinovski, L., Wilchek, M., Mirelman, D., & Weiner, L. (1998). The mode of action of allicin: trapping of radicals and interaction with thiol containing proteins. Biochimica Et Biophysica Acta - General Subjects, 1379(2), 233–244. https://doi.org/10.1016/s0304-4165(97)00104-9

[68] Structure of Allicin: https://pubchem.ncbi.nlm.nih.gov/compound/65036

[69] Rahman NA, Fazilah A, Effarizah ME (2015). "Toxicity of Nutmeg (Myristicin): A Review". International Journal on Advanced Science, Engineering and Information Technology. 5 (3): 212–215. CiteSeerX 10.1.1.920.6379. doi:10.18517/ijaseit.5.3.518

[70] Lichtenstein EP, Casida JE (1963). "Naturally Occurring Insecticides, Myristicin, an Insecticide and Synergist Occurring Naturally in the Edible Parts of Parsnips". Journal of Agricultural and Food Chemistry. 11 (5): 410–415. doi:10.1021/jf60129a017

[71] Srivastava S, Gupta MM, Prajapati V, Tripathi AK, Kumar S (2001). "Insecticidal Activity of Myristicin from Piper mullesua". Pharmaceutical Biology. 39 (3): 226–229. doi:10.1076/phbi.39.3.226.5933. S2CID 83947896.

[72] Clark CR, DeRuiter J, Noggle FT (1996-01-01). "Analysis of 1-(3-Methoxy-4,5-Methylenedioxyphenyl)-2-Propanamine (MMDA)Derivatives Synthesized from Nutmeg Oil and 3-Methoxy-4,5-Methylenedioxybenzaldehyde". Journal of Chromatographic Science. 34 (1): 34–42. doi:10.1093/chromsci/34.1.34.

[73] Stein U, Greyer H, Hentschel H (April 2001). "Nutmeg (myristicin) poisoning--report on a fatal case and a series of cases recorded by a poison information centre". Forensic Science International. 118 (1): 87–90. doi:10.1016/s0379-0738(00)00369-8. PMID 11343860

[74] Lee, B. R., Kim, J. N., Jung, J. Y., Choi, J., Han, E. J., Lee, S. S., Ko, K. H., & Ryu, J. H. (2005). Myristicin-induced neurotoxicity in human neuroblastoma SK-N-SH cells. Toxicology Letters, 157(1), 49–56. https://doi.org/10.1016/j.toxlet.2005.01.012

[75] Yang, A., He, X., Chen, J., He, L., Jin, C., Wang, L., Zhang, F., & An, L. (2015). Identification and characterization of reactive metabolites in myristicin-mediated mechanism-based inhibition of CYP1A2. Chemico-Biological Interactions, 237, 133–140. https://doi.org/10.1016/j.cbi.2015.06.018

[76] Seneme, E. F., Santos, D. R. D., Silva, E., Franco, Y. E. M., & Longato, G. B. (2021). Pharmacological and Therapeutic Potential of Myristicin: A Literature Review. Molecules, 26(19), 5914. https://doi.org/10.3390/molecules26195914

[77] Structure of Myristicin: https://pubchem.ncbi.nlm.nih.gov/compound/4276

[78] Majeed S (28 December 2015). "The State of the Curcumin Market". Natural Products Insider

[79] Salem, M., Rohani, S., & Gillies, E. R. (2014). Curcumin, a promising anti-cancer therapeutic: a review of its chemical properties, bioactivity and approaches to cancer cell delivery. RSC Advances, 4(21), 10815. https://doi.org/10.1039/c3ra46396f

[80] Ak, T. P., & Gülçin, İ. (2008). Antioxidant and radical scavenging properties of curcumin. Chemico-Biological Interactions, 174(1), 27–37. https://doi.org/10.1016/j.cbi.2008.05.003

[81] Srimal, R. C., & Bn, D. (2011). Pharmacology of diferuloyl methane (curcumin), a non-steroidal anti-inflammatory agent. Journal of Pharmacy and Pharmacology, 25(6), 447–452. https://doi.org/10.1111/j.2042-7158.1973.tb09131.x

[82] Tomeh, M. A., Hadianamrei, R., & Zhao, X. (2019). A Review of Curcumin and Its Derivatives as Anticancer Agents. International Journal of Molecular Sciences, 20(5), 1033. https://doi.org/10.3390/ijms20051033

[83] Vareed, S. K., Kakarala, M., Ruffin, M. T., Crowell, J. A., Normolle, D. P., Djuric, Z., & Brenner, D. E. (2008). Pharmacokinetics of Curcumin Conjugate Metabolites in Healthy Human Subjects. Cancer Epidemiology, Biomarkers & Prevention, 17(6), 1411–1417. https://doi.org/10.1158/1055-9965.epi-07-2693

[84] Structure of Curcumin: https://pubchem.ncbi.nlm.nih.gov/compound/969516

[] Burley, S. K., Berman, H. M., Bhikadiya, C., Bi, C., Chen, L., Caruso, U., Christie, C., Duarte, J. M., Dutta, S., Feng, Z., Ghosh, S., Goodsell, D. S., Green, R., Guranovic, V., Guzenko, D., Hudson, B., Liang, Y., Lowe, R., Peisach, E., . . . Ioannidis, Y. (2019). Protein Data Bank: the single global archive for 3D macromolecular structure data. Nucleic Acids Research, 47(D1), D520–D528. https://doi.org/10.1093/nar/gky949

[85] El-Hachem, N., Haibe-Kains, B., Khalil, A., Kobeissy, F., & Nemer, G. (2017). AutoDock and AutoDockTools for Protein-Ligand Docking: Beta-Site Amyloid Precursor Protein Cleaving Enzyme 1(BACE1) as a Case Study. In Methods in molecular biology (pp. 391–403). Springer Science+Business Media. https://doi.org/10.1007/978-1-4939-6952-4_20

[86] Mgl-Admin. (n.d.-b). Homepage. AutoDock. https://autodock.scripps.edu/

[87] Morris, G. M., Huey, R., Lindstrom, W. M., Sanner, M. F., Belew, R. K., Goodsell, D. S., & Olson, A. J. (2009). AutoDock4 and AutoDockTools4: Automated docking with selective receptor flexibility. Journal of Computational Chemistry, 30(16), 2785–2791. https://doi.org/10.1002/jcc.21256

[88] Huey, R., Morris, G. M., Olson, A. J., & Goodsell, D. S. (2007). A semiempirical free energy force field with charge-based desolvation. Journal of Computational Chemistry, 28(6), 1145–1152. https://doi.org/10.1002/jcc.20634

[89] Burley, S. K., Berman, H. M., Bhikadiya, C., Bi, C., Chen, L., Caruso, U., Christie, C., Duarte, J. M., Dutta, S., Feng, Z., Ghosh, S., Goodsell, D. S., Green, R., Guranovic, V., Guzenko, D., Hudson, B., Liang, Y., Lowe, R., Peisach, E., . . . Ioannidis, Y. (2019). Protein Data Bank: the single global archive for 3D macromolecular structure data. Nucleic Acids Research, 47(D1), D520–D528. https://doi.org/10.1093/nar/gky949.